Università degli Studi di Cagliari

PHD DEGREE

……Scienze della vita dell'ambiente e del farmaco……

Cycle ……XXX……...

TITLE OF THE PHD THESIS

…Evaluation of natural compounds for inflammatory diseases and their improvement by nanoencapsulation in phospholipid systems...

Scientific Disciplinary Sector(s)

…… CHIM/09 (Farmaceutico Tecnologico Applicativo)……

PhD Student: …Ana Catalán Latorre…

Coordinator of the PhD Programme …Enzo Tramontano……

Supervisor …Maria Manconi.....

Final exam. Academic Year 2016 – 2017
Thesis defence: February-March 2018 Session

Evaluation of natural compounds for inflammatory diseases and their improvement by nanoencapsulation in phospholipid systems

Introduction

Pollution, poor nutrition, insufficient physical activity, and the use of tobacco and alcohol are the primary cause of most chronic and aging-related diseases. These factors produce an excess of reactive oxygen species leading a pro-oxidative condition in the human body. When an overload of these free radicals cannot be gradually destroyed by endogenous antioxidants, its accumulation generates a phenomenon called oxidative stress. This process negatively affects the equilibrium of local gut microbiota and leads to systemic oxidative damage of cellular biomolecules (lipids, proteins and nucleic acids), thus, playing a major role in the development of chronic and degenerative illness such as cancer, autoimmune disorders, aging, cataract, rheumatoid arthritis, cardiovascular and neurodegenerative diseases. Recent evidence suggests the linking of the status of human gut microbiome to both health improvement and the development of various diseases. Beneficial bacteria (e.g., Bifidobacterium, Lactobacillus) ensure the barrier function of intestinal membrane against pathogens; stimulate the host immune system; prevent food allergies and tumours; produce vitamins; metabolize cholesterol and other lipids; and enhance mineral bioavailability [1,2]. Conversely, the overgrowth of deleterious bacterial species (e.g., some Clostridium) causes chronic and acute bowel diseases and influence the development of comorbidities associated with aging, cancer and degenerative diseases. Manipulation of the microbiota and microbiome holds promise as an innovative strategy to favorably promote or support the host health.

Also, antioxidants play a key role in attenuate oxidative responses in local or systemic conditions and their beneficial responses have the potential to increase life expectancy. They are produced from normal cell metabolisms in situ or incorporated from external sources (i.e. dietary intake). Phenolic compounds and other natural molecules represent an important source of antioxidants in the diet. They are ubiquitous in plant species and are able to cope with oxidative stress, thus playing a key role in the protection of human health [3].

Since the in vivo bioavailability of such molecules is usually limited by poor water solubility and high instability, their efficacy can be improved by incorporation in suitable nanocarries. Recently, new types of products based on natural molecules loaded in technological nanoparticles have been developed and proposed as integrative food, cosmetic and therapeutic formulations. Due to the high costs and complex preparation methods, such delivery systems are commonly applied in drug delivery with only few therapeutic formulations currently on the market. In addition, no cosmeceutical and nutraceutical products containing natural molecules are currently marketed though nanosystems. This target represents a new frontier in both cosmeceutical and nutraceutical fields, which can take advantage of natural resources to obtain food, cosmetic and nutraceutical products. Additionally, these highly performant phytonanoformulations could be specifically designed using only environmentally-friendly, scalable methods and biocompatible ingredients. In fact, nowadays there is a large demand for such natural, eco-green and beneficial products as alternative of traditional medicaments. Consumers prefer functional foods, cosmetics and nutraceutical products based on nutrients and natural bio-active compounds capable of beneficial effects under physio-pathological conditions. Both nutraceutical and functional food markets have grown and are expanding worldwide as a consequence of a rising global consumer demand for all-natural functional ingredients by health conscious consumers.

Taking into account these findings, in the present PhD thesis new and environmentally-friendly phospholipid vesicles have been developed and tested as carrier to the intestinal delivery of a potent

natural antioxidant, the curcumin. Curcumin (CUR) is one of the most widely distributed flavonoids and has demonstrated to possess potent anti-oxidant, anti-inflammatory and anti-carcinogenic activities. It controls the formation of proinflammatory mediators, such as prostaglandins and leukotrienes. It aids in the management of oxidative and inflammatory conditions, metabolic syndrome, arthritis, anxiety, and hyperlipidemia [4]. Curcumin was loaded in phospholipid vesicles especially designed for intestinal delivery.

Freeze-dried eudragit-hyaluronan multicompartment liposomes to improve the intestinal bioavailability of curcumin

1. INTRODUCTION

Curcumin is the main ingredient of turmeric spice, derived from the rhizomes of *Curcuma longa*. It is a polyphenol traditionally used in Asia as nutritional supplement and natural remedy . Recent studies support its beneficial effect in a wide range of affections, such as early aging, oxidative stress, acute or chronic inflammation, cardiovascular and neurodegenerative pathologies [3–9]. Several curcumin-based products are available on the market as dietary supplements, by virtue of the antioxidant properties and safety profile (curcumin has GRAS status). Further, curcumin has been widely explored as a pharmacological agent in nanomedicine, due to its high activity *in vitro* and despite the low systemic bioavailability *in vivo* [10]. It is poorly soluble in water, scarcely stable under physiological conditions, inadequately absorbed, and rapidly removed from the body. Moreover, its strong interaction with bile salts alters the intestinal absorption, as previously demonstrated [11]. In recent years, many efforts have been made to increase the potential of curcumin for health promotion and disease prevention, by improving its bioavailability. A large number of research works have focused on innovative formulations intended for oral, pulmonary and topical delivery of curcumin, using innovative ingredients or carrier systems specific for the selected target [12–14]. The oral administration of curcumin in innovative carriers represents the most attractive strategy, because it can ensure local delivery and accumulation in the intestines, and improve the systemic biovailability at the same time [15,16]. Nanoparticulate systems are promising tools for oral delivery of low bioavailable compounds, when properly designed [17–19]. Among the different nanosystems, liposomes have been widely employed due to their safety and versatility. The incorporation of curcumin in phospholipid vesicles can modulate its accumulation in the intestines and the interaction with the intestinal mucosa, but these systems cannot ensure drug stability in the gastrointestinal environment, due to the phospholipid degradation under such

conditions [20,21]. Li et al. formulated flexible liposomes, which were modified on the surface using silica to enhance their stability and structural integrity against the hostile bioenvironment encountered after oral administration. The silica-coated liposomes effectively improved the stability of flexible liposomes, confirming the key role of the polymer around the liposomal surface [22]. The same approach was used by Chen et al., which found that the trymethil-chitosan polymer on the liposomal surface improved the stability and the oral bioavailability of curcumin. However, both systems were obtained using organic solvents and a complex, multistep preparation method [23]. The appropriate combination of phospholipids with gastroresistant polymers can offer protection to the vesicles, resulting in an enhanced local and systemic bioavailability of the loaded drug. Hence, in this work, Eudragit® S100, a gastroresistant polymer, was used to protect the vesicles from the gastric pH, and, for the first time, it was combined with hyaluronan to immobilize the phospholipid structures, by using an eco-friendly preparation method previously used to obtain hyalurosomes [24]. Sodium hyaluronate was selected because of its solubility in water, and at pH>3 its acid chains are extensively ionized forming strong intermolecular interactions, with a consequent development of a structured network with peculiar visco-elastic properties [24]. To optimize the formulation, Eudragit® S100 was solubilized in ethanol with curcumin and mixed, at different ratios, with hyaluronan and curcumin dispersed in water. As previously reported for hyalurosomes, the curcumin-polymer dispersions were used as hydrating medium for the phospholipid, and the resulting systems were freeze-dried and rehydrated with water prior to use [24]. Four different formulations of curcumin-loaded polymer immobilized vesicles were prepared and characterized. The ability of the vesicles to withstand ionic strength and acidic/neutral pH was tested *in vitro*, along with their carrier performances for the improvement of the intestinal deposition of curcumin *in vivo*, and the protection of cells against oxidative stress.

2. MATERIALS AND METHODS

Materials

Soy phosphatidylcholine (Phospholipon® 90G, P90G) was purchased from Lipoid GmbH (Ludwigshafen, Germany). Sodium hyaluronate or hyaluronan (HY) low molecular weight (200-400 kDa) was purchased from DSM Nutritional Products AG Branch Pentapharm (Aesch, Switzerland). Eudragit® S100 (EU) with molecular weight about 125 kDa was provided by Evonik Industries AG (Darmstadt, Germany). Curcumin, ethanol and other reagents of analytical grade were purchased from Sigma-Aldrich (Milan, Italy). Cell medium, foetal bovine serum, penicillin, and streptomycin were purchased from Life Technologies Europe (Monza, Italy).

Sample preparation

The following drug-polymer dispersions were prepared: A) curcumin (100 mg) and hyaluronan (50 mg) in 10 ml of bidistilled water; B) curcumin (100 mg) and Eudragit® S100 (500 mg) in 10 ml of ethanol; C) curcumin (100 mg) and Eudragit® S100 (250 mg) in 10 ml of ethanol. All dispersions were stirred for 2 h, at 25°C. Dispersion A (1 or 1.5 ml) was mixed with dispersion B (1 or 0.5 ml) or dispersion C (1 or 0.5 ml) to obtain 2 ml of four different hydrating media. In a typical formulation, 2 ml of such media was added to 180 mg of P90G, left hydrating overnight and sonicated (25 cycles, 5 seconds on and 2 seconds off, 13 microns of probe amplitude) with a high intensity ultrasonic disintegrator (Soniprep 150, MSE Crowley, London, UK) [25]. The resulting vesicle dispersions were frozen at −80°C and freeze-dried for 24 h at -80°C and 0 mm Hg, using a Freeze-Dryer Criotecnica, (AMCOTA, Rome, Italy) [26]. Each sample was rehydrated with 2 ml of bidistilled water and sonicated (50 cycles, 5 seconds on and 2 seconds off) prior to use. The composition of the four formulations is reported in Table 1.

Table 1. Composition of the hyaluronan-Eudragit-phospholipid complex vesicles.

sample	P90G (mg/ml)	Curcumin (mg/ml)	Hyaluronan (mg/ml)	Eudragit (mg/ml)
HY2EU25 liposomes	90	10	2.50	25.00
HY3EU12 liposomes	90	10	3.75	12.50
HY2EU12 liposomes	90	10	2.50	12.50
HY3EU6 liposomes	90	10	3.75	6.25

Vesicle characterization

Vesicle formation and morphology were evaluated by cryo-TEM analysis. A thin film of each sample was formed on a holey carbon grid and vitrified by plunging (kept at 100% humidity and room temperature) into ethane, maintained at its melting point, using a Vitrobot (FEI Company, Eindhoven, The Netherlands). The vitreous films were transferred to a Tecnai F20 TEM (FEI Company), and the samples were observed in a low dose mode. Images were acquired at 200 kV at a temperature ~ -173°C, using low-dose imaging conditions with a CCD Eagle camera (FEI Company).

The average diameter and polydispersity index (PI; a measure of the size distribution width) were determined by Photon Correlation Spectroscopy (PCS) using a Zetasizer nano-ZS (Malvern Instruments, Worcestershire, UK). Samples were backscattered by a helium-neon laser (633 nm) at an angle of 173° and a constant temperature of 25°C. Zeta potential was estimated using the Zetasizer nano-ZS by means of the M3-PALS (Mixed Mode Measurement-Phase Analysis Light Scattering) technique, which measures the particle electrophoretic mobility. Prior to analysis, the samples (100 μl) were diluted with water (10 ml). Entrapment efficiency (EE) was calculated as the percentage of the drug amount found after dialysis versus that initially used. Samples (1 ml) were purified from the non-incorporated drug by dialysis against water (2.5 l) using dialysis tubing (Spectra/Por® membranes, 12–14 kDa MW cut-off, 3 nm pore size; Spectrum Laboratories Inc., DG Breda, The Netherlands) at 20°C for 4 h, refreshing water every hour. The water used (10 l total)

was theoretically able to remove the drug present in 1 ml of dispersion (10 mg). The amount of curcumin in each dispersion was determined at 424 nm using a UV spectrophotometer (Lambda 25, Perkin Elmer, USA) after disruption of the vesicles with methanol (1:1000).

Vesicle behaviour in gastrointestinal fluids

The average diameter, polydispersity index and zeta potential of the vesicles were measured after dilution (1:100 v:v) and incubation at pH 2 for 2 h and at pH 7 for 6 h, at 37°C, in the presence of sodium chloride (0.3 M), which was used to increase the ionic strength in the media. The parameters were measured immediately after dilution of the vesicles with the media, and after 2 or 6 h.

Activity of curcumin loaded vesicles against oxidative stress

The *in vitro* antioxidant activity (AA%) of curcumin loaded vesicles was measured by the DPPH (2,2-diphenyl- 1-picrylhydrazyl) assay. Each dispersion (10 μl) was dissolved in 1990 μl of DPPH methanolic solution (40 μg/ml). The sample was incubated for 30 min at room temperature, in the dark. Then, the absorbance was measured at λ = 517 nm against blank. All the experiments were performed in triplicate. The AA% was calculated according to the following formula:

$AA\% = [(ABS_{DPPH} - ABS_{sample})/ABS_{DPPH}] \times 100$.

The antioxidant activity of curcumin loaded vesicles was also assessed in cell culture. Caco-2 cells were grown as monolayer in 35-mm tissue culture dishes, at 37°C in humidified atmosphere of 5% CO_2 in air. Dulbecco's Modified Eagle Medium high glucose, containing L-glutamine, supplemented with 20% foetal bovine serum (FBS), penicillin/streptomycin and fungizone, was used as growth medium. The cells were seeded into 96-well plates at a density of 7.5×10^3 cells/well. After 24 h of incubation, the cells were treated for 4 h with hydrogen peroxide (1:50000) and the curcumin in aqueous dispersion or loaded in vesicles (final concentration of curcumin 0.02 mg/ml). Cells treated with hydrogen peroxide-only were used as a positive control. After 4 h of incubation, the cells were washed with fresh medium, and their viability was determined by the MTT [3(4,5-dimethylthiazolyl-2)-2, 5-diphenyltetrazolium bromide] colorimetric assay, adding 200 μl of MTT

reagent (0.5 mg/ml in PBS) to each well. After 2 h, the formed formazan crystals were dissolved in DMSO and their concentration was spectrophotometrically quantified at 570 nm with a microplate reader (Synergy 4, Reader BioTek Instruments, AHSI S.p.A, Bernareggio, Italy). The results are reported as the percentage of untreated cells (100% viability).

In vivo intestinal biodistribution of curcumin

In vivo studies were performed in accordance with European Union regulations for the handling and use of laboratory animals. Wistar male rats, aged 8-12 weeks and weighing 230-250 g, were housed in air-conditioned rooms at 22±3°C, 55±5% humidity, 12 h light/dark cycles and allowed free access to water and chow for the duration of the studies. Curcumin dispersion or curcumin-loaded vesicles (2 ml) were intragastrically administered to healthy rats (at least 4 for each group) by gavage. After 3 h, rats were sacrificed and liver, kidneys and intestines were excised. The intestines were emptied and divided in segments (duodenum, jejunum, cecum and colon), slightly stretched and carefully spread on a dissecting board and photographed. The specimens were soaked in acetonitrile:water (70:30, v/v), homogenized and centrifuged at 12500 rpm for 10 min. The amount of curcumin was quantified by HPLC using a chromatograph (Thermo Scientific, Madrid, Spain) equipped with a C_{18} Novapak column (Waters, Madrid, Spain). The mobile phase consisted of a mixture of acetonitrile/water/acetic acid (50:49:1, v/v/v), delivered at a flow rate of 1 ml/min, and detection was performed at 425 nm. Results were expressed as the ratio of the amount of curcumin in the organ versus the amount of curcumin administered.

Statistical analysis of data

Results are expressed as the mean±standard deviation. Analysis of variance (ANOVA) was used to evaluate multiple comparison of means and Tukey's test and Student's t-test were performed to substantiate differences between groups using XLStatistics for Windows. The differences were considered statistically significant for $p<0.05$.

3. RESULTS

Vesicle preparation and characterization

Eudragit® S100 is an anionic copolymer able to form an effective and stable enteric coating with a fast dissolution in the upper bowel. It is poorly soluble in water and when added to the phospholipid and curcumin, the resulting vesicles were large (>800 nm) and polydispersed (>0.80). Hence, Eudragit® S100 was dispersed in ethanol with curcumin (dispersion B or C) and mixed with the curcumin-hyaluronan dispersion in water (dispersion A). The resulting dispersions appeared homogeneous, without drug aggregates or precipitate, indicating the contribution of the polymers to the dissolution of curcumin [15]. By combining dispersion A with different ratios of dispersion B or C (1:1 or 1.5:0.5) and using them as hydrating medium of the phospholipid, four different formulations were obtained, all having similar characteristics: approximately 400 nm in size and PI <0.4 ($p>0.05$ among groups). The vesicles were freeze-dried to eliminate the solvent and then rehydrated with water, prior to use. The freeze-drying process led to a reduction of vesicle size and a greater homogeneity of the system, indicating the formation of more suitable structures where the polymers played a key role in vesicle assembly and curcumin loading (Figure 2). Indeed, curcumin loaded liposomes without the polymers were large in size (≥700 nm), polydispersed (≥0.70) and not stable, with drug precipitation. On the contrary, the size of eudragit-hyaluronan immobilized liposomes ranged from 220 to 287 nm, and seemed to be mostly affected by the hyaluronan concentration and less by the Eudragit® S100 concentration: liposomes with 25 and 12.5 mg/ml of Eudragit® S100 and the same amount of hyaluronan (2.5 mg/ml) were of equal size (~280 nm, $p>0.05$), while vesicles with a slightly higher amount of hyaluronan (3.75 mg/ml) were smaller ($p<0.05$), regardless of the amount of Eudragit® S100 used. The zeta potential was highly negative for all the samples, thus ensuring vesicle stability in dispersion [27]. The entrapment efficiency was very similar for all the samples ($p>0.05$), ranged from 78% to 82%, indicating a good ability to load and retain the lipophilic molecule.

The vesicle structure and morphology were evaluated by cryo-TEM (Figure 1). In agreement with PCS results, the vesicles were irregularly sized and shaped: they were spherical or oval, multilamellar or large unilamellar vesicles with 1 to 4 small vesicles inside (multicompartment vesicles).

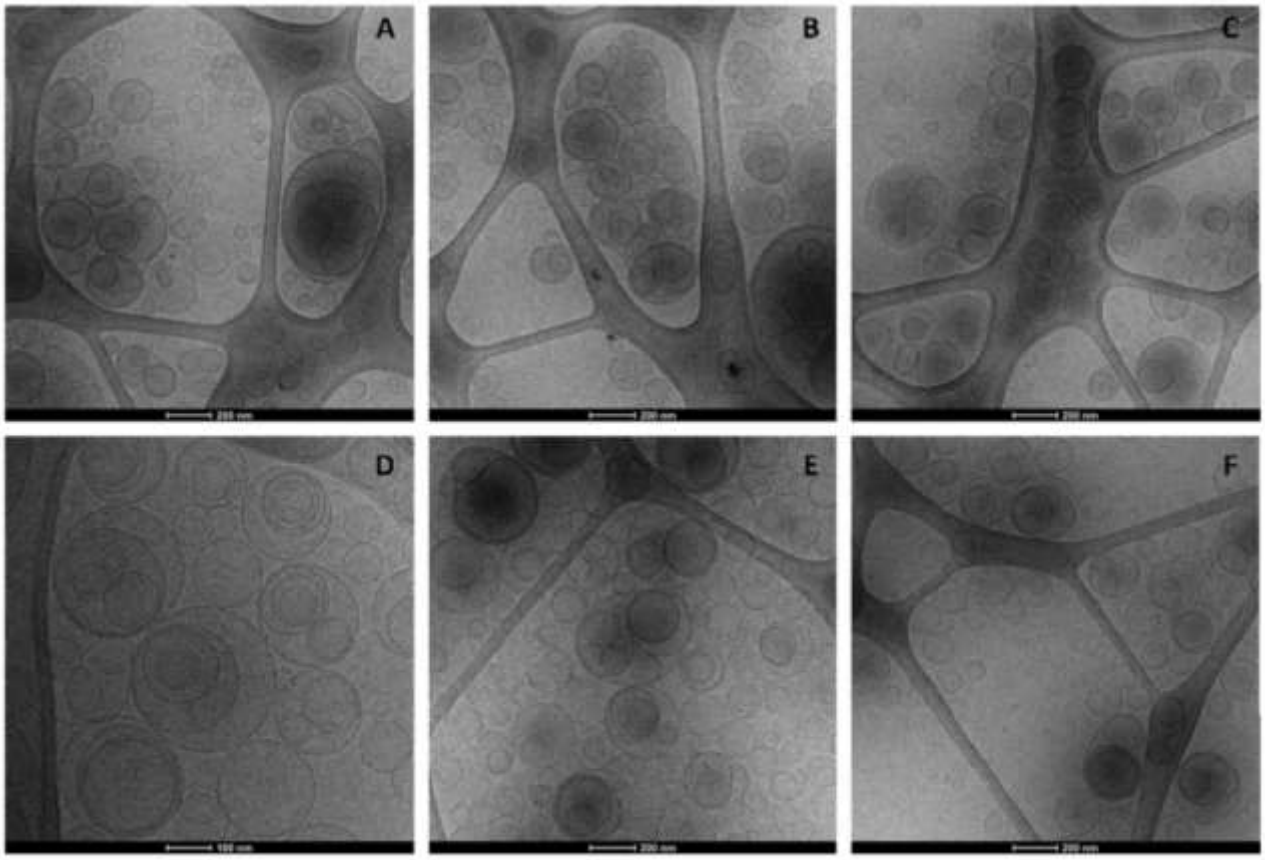

Figure 1. Representative cryo-TEM images of curcumin loaded eudragit-hyaluronan immobilized vesicles: HY2EU25 liposomes (A), HY3EU12 liposomes (B), HY2EU12 liposomes (C), HY3EU6 liposomes (D).

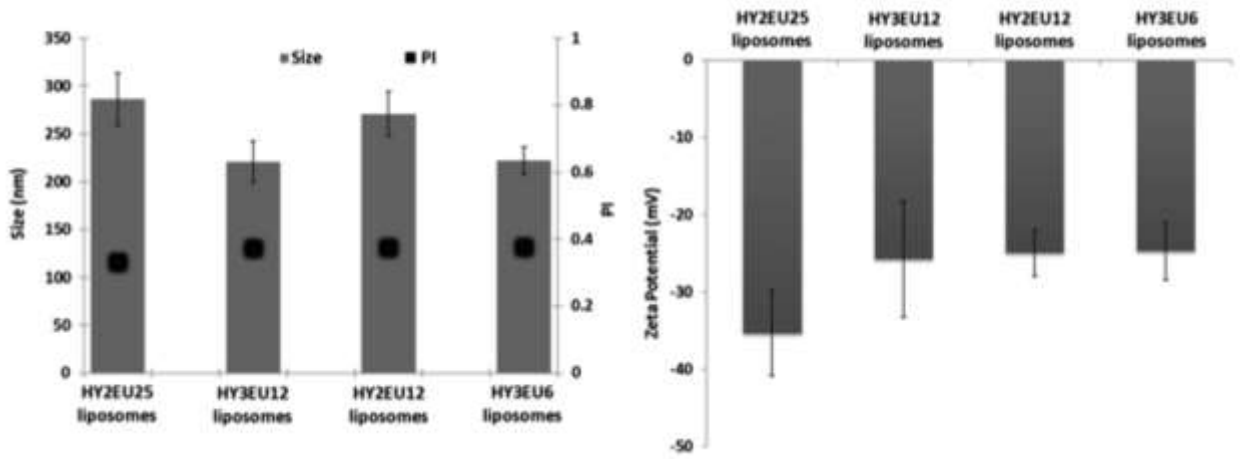

Figure 2. Average size, polydispersity index (PI) and zeta potential of eudragit-hyaluronan immobilized liposomes. Bars represent standard deviations (n= 6).

The freeze-dried samples were analysed by X-ray diffraction to evaluate the polymer/phospholipid/drug interactions (Figure 3). XRD patterns of hyaluronan and Eudragit® S100 show a broad halo without long range order of crystalline materials, thus indicating their amorphous state. The phospholipid (P90G) showed the typical pattern of lipids, characterized by a diffused halo centred at 20° 2ϑ and several narrow peaks at 3.91, 5.74, 7.57, 9.40, 11.36, 13.18 and 15.01° 2ϑ. The pattern of curcumin presented a series of sharp peaks, which indicate its microcrystalline state. These peaks were partially visible in the spectrum of the physical mixture (at 9.0 and 17.5° 2ϑ), together with those of the phospholipid. The spectra of eudragit-hyaluronan immobilized liposomes were very similar to that of the phospholipid, without the characteristic peaks of curcumin, indicating the amorphization of the drug in the formulations.

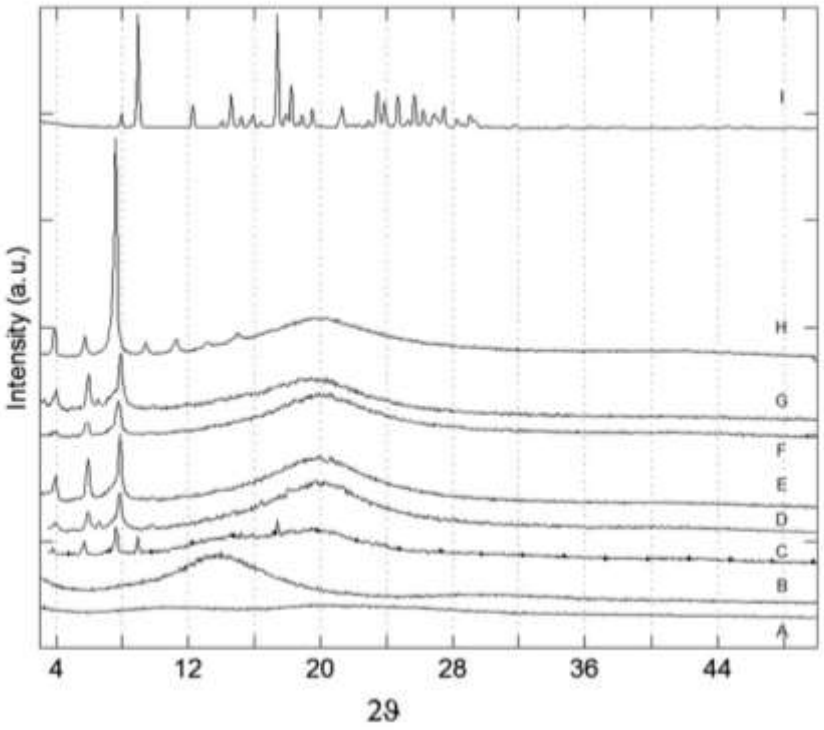

Figure 3. X-ray diffraction patterns of hyaluronan (A), Eudragit® S100 (B), physical mixture of the raw components (C), HY2EU25 liposomes (D), HY3EU12 liposomes (E), HY2EU12 liposomes (F), HY3EU6 liposomes (G), P90G (H), curcumin (I).

Vesicle behaviour in gastrointestinal fluids

Since oral formulations are subjected to pH and ionic strength variations along the gastrointestinal tract, the behaviour of the different liposomal formulations under conditions mimicking stomach-to-colon transit was evaluated using two media at pH 2 and pH 7, with high ionic strength (Table 2). The size of the vesicles did not vary significantly ($p>0.05$ *vs.* starting values) after 2 h at acidic pH and 6 h at neutral pH, regardless of the ratio of Eudragit® S100 and hyaluronan, confirming the ability of the vesicle to preserve their structure despite the ionic strength and pH of the medium, thanks to the polymeric combination. Only a slight increase in polydispersity and zeta potential (less negative) was observed in both media.

Table 2. Average size, polydispersity index (PI) and zeta potential (ZP) of the vesicle formulations diluted and incubated at 37°C at pH 2 and pH 7. The measurements were carried out immediately after the dilution (t_0) and after 2 h at pH 2 (t_{2h}) or 6 h at pH 7 (t_{6h}).

Sample	time	size±SD (nm)		PI		ZP±SD (mV)	
		pH 2	pH 7	pH 2	pH 7	pH 2	pH 7
HY2EU25 liposomes	t_0	289±8	274±10	0.46	0.38	-13±3	-5±1
	$t_{2/6h}$	290±18	274±19	0.45	0.35	-18±2	-6±1
HY3EU12 liposomes	t_0	254±17	228±14	0.36	0.42	-22±4	-4±1
	$t_{2/6h}$	234±15	224±7	0.44	0.32	-18±5	-5±1
HY2EU12 liposomes	t_0	238±21	224±14	0.54	0.38	-5±4	-12±1
	$t_{2/6h}$	258±12	244±10	0.43	0.36	-8±5	-13±1
HY3EU6 liposomes	t_0	180±18	176±10	0.37	0.28	-23±5	-4±1
	$t_{2/6h}$	195±16	175±19	0.35	0.28	-13±5	-4±1

Activity of curcumin loaded vesicles against oxidative stress

In line with the well-known antioxidant activity of curcumin, all the prepared formulations showed a great ability to scavenge DPPH free radical, similarly to curcumin dispersion (~90%; $p>0.05$). Additionally, the ability of liposomes to protect Caco-2 intestinal cells from oxidative stress induced by hydrogen peroxide was evaluated (Figure 4). The exposure to hydrogen peroxide led to a significant reduction of cell viability, reaching ~50% with respect to untreated cells (negative control). The curcumin aqueous dispersion (0.020 mg/ml), despite having the same antioxidant activity *in vitro,* was not able to effectively counteract the damages caused by hydrogen peroxide, as the viability was ~57% ($p>0.05$ *vs.* positive control). The protective effect of curcumin was greatly enhanced by its incorporation in polymer immobilized vesicles, which provided almost complete restoration of healthy conditions, as the viability was ~95% ($p>0.05$ among the formulations).

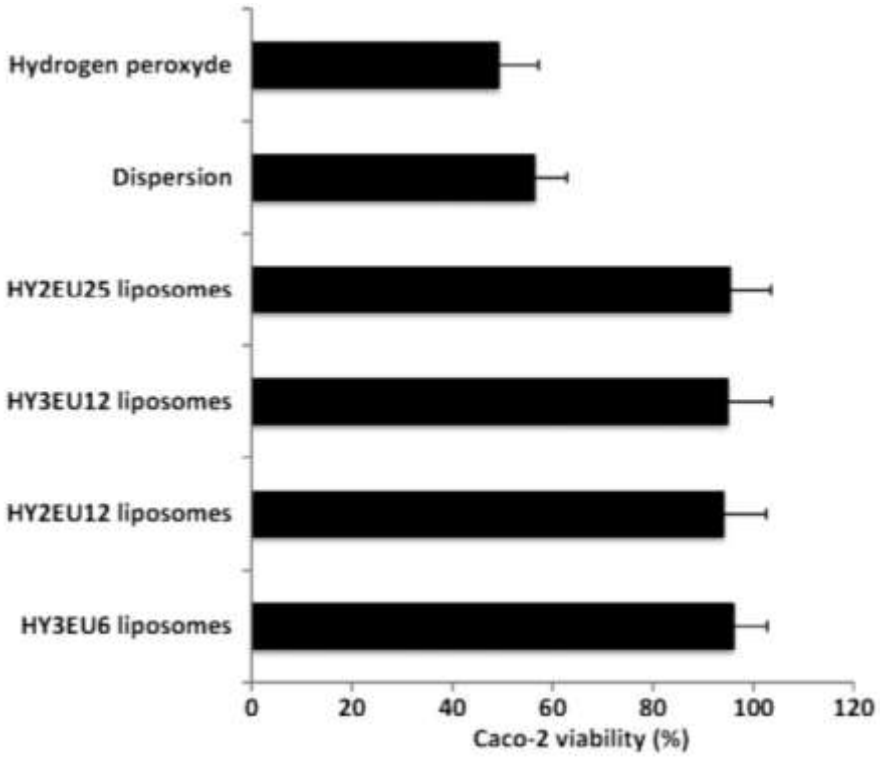

Figure 4. Viability of Caco-2 cells exposed to hydrogen peroxide alone or simultaneously treated with curcumin aqueous dispersion or curcumin loaded eudragit-hyaluronan immobilized liposomes. Data are reported as mean values ± standard deviation (error bars) of cell viability expressed as the percentage of the negative control (100% viability).

***In vivo* curcumin biodistribution in the intestines**

Due to the similarity of formulations in terms of physico-chemical characteristics and *in vitro* performances, the *in vivo* studies were carried out by using only HY2EU25 liposomes and HY2EU12 liposomes (Table 1), which had the same amount of hyaluronan and the highest amounts of Eudragit® S100. The polymer is insoluble in acidic environment, thus being gastro-resistant, and in the selected formulations is expected to ensure the highest stability of the vesicles during the passage through the stomach. *In vivo* biodistribution results showed that the amount of curcumin found in liver and kidneys was negligible, while the local accumulation in the intestines was

favored. The intestine of rats treated with eudragit-hyaluronan immobilized liposomes showed yellow coloring, due to the higher accumulation of curcumin (Figure 5).

Figure 5. Photographs of excised intestines of rats, 3 h after the administration of curcumin dispersion or curcumin loaded eudragit-hyaluronan immobilized liposomes.

This macroscopic result was confirmed by extraction and quantification of curcumin by HPLC. The vesicles provided a higher curcumin deposition in all the intestine tracts, as compared to that obtained with the dispersion ($p<0.05$; Figure 6). In particular, after the administration of the dispersion, the amount of curcumin in the jejunum was ~5% of the administered dose, while using HY2EU25 liposomes it was four-fold higher (~20%), and using HY2EU12 liposomes reached ~25%. Moreover, after the administration of the dispersion, the amount of curcumin found in the colon was negligible, while it was ~3% after the administration of liposomes.

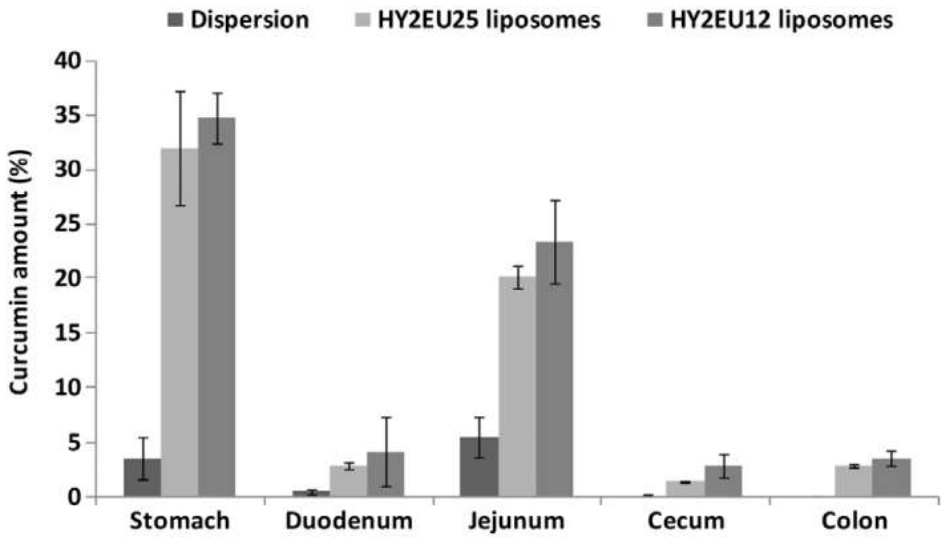

Figure 6. Amount (%) of curcumin found in different parts of the gastrointestinal tract, 3 h after its administration in dispersion or in eudragit-hyaluronan immobilized liposomes. Data are reported as mean values ± standard deviation (error bars).

4. DISCUSSION

Electrostatic interactions with external ions play an important role in the stability of liposomes, as they can cause an alteration of the structure and size, with possible rupture and content leakage [24,25]. Several studies focused on the assessment of the influence of gastrointestinal conditions, such as pH and ionic strength, on vesicle stability, underlining their low resistance and feasible breaking. In an attempt to overcome this limitation, phospholipid vesicles have been developed by using different natural polymers, such as chitosan, sodium alginate, xanthan gum, gelatin pectin and cellulose ethers [28,30,31]. Further, liposomes have been coated with the methacrylic acid copolymer Eudragit® S100 to improve the vesicle stability towards environmental stress [32]. This polymer, based on methacrylic acid and methyl methacrylate (1:1 ratio), is soluble at pH 7 and insoluble at lower pH values. For the first time, in this work, Eudragit S100® was combined with hyaluronan to immobilize phospholipid vesicles, improve their stability and promote curcumin deposition in the intestines. Moreover, the vesicles were prepared using an easy and

environmentally-friendly method already proposed for hyalurosomes, with some modifications that allowed the formulation upgrading [24]. The curcumin-polymer dispersion was used to hydrate the phospholipid, and the resulting vesicles were freeze-dried and rehydrated, providing better curcumin, polymer, phospholipid interactions [33]. The combination of Eudragit® S100 and hyaluronan dramatically affected the vesicles, facilitating their assembly and curcumin loading, while liposomes without the polymers were not suitable for pharmaceutical applications, as they were large in size (≥700 nm), polydispersed (≥0.70) and unstable, displaying drug precipitation in a short time. It is likely that the polymers, by interacting with each other and with the phospholipid, produced a polymer network in which both the vesicles and the drug were embedded and stabilized, with a consequent improvement of the loading and retention of curcumin [15,24]. The combined polymers favoured the dispersion of curcumin in the formulations after freeze-drying, and the vesicles rearranged easily upon rehydration with water. Considering that the long-term stability of vesicles in dispersion represents one of the major limitations to their commercial application, this technique offers a solution to the instability issues, preserves the carrier's performances, and allows the easy re-dispersion of the freeze-dried liposomes prior to use. Additionally, during the vesicle rehydration process, the lamellae close themselves to form closed compartments, which surround smaller vesicles, forming multicompartment structures.

The combined polymers were able to protect the vesicles from the harsh conditions of the gastrointestinal tract, such as high ionic strength and pH variations, preserving their structure. Thanks to this resistance and to the peculiar multicompartment structure, eudragit-hyaluronan immobilized liposomes provided a greater deposition of curcumin in the intestines, with respect to the dispersion. The results suggest that the combination of the polymers increased the stability of the vesicle in the gastric environment, allowing the intact vesicles to reach the intestines and adhere to the mucosal surface where the external bilayer of the multicompartment vesicles fuse, freeing the inner vesicles, which penetrate the membrane and release curcumin.

The effect of the polymer immobilized liposomes on the antioxidant activity of curcumin was also studied. Its ability to scavenge the DPPH free radical was not affected by the incorporation in the vesicles, while its efficacy in the inhibition of hydrogen peroxide cell damage was even strengthened, regardless of the eudragit-hyaluronan ratio. This is probably due to the ability of the system to interact with cells favouring the internalization of curcumin, which may exert its antioxidant activity in the intracellular environment, thus, preventing oxidative damage and consequent cell death.

5. CONCLUSION

In the present work, innovative multicompartment vesicles was produced by combining Eudragit® S100 and hyaluronan with curcumin and a phospholipid, by using an easy and environmentally-friendly method. The vesicles showed promising properties for the intestinal delivery of curcumin, by protecting the polyphenol from the gastric environment and favoring its local accumulation in the intestines, where it can exert its antioxidant activity.

Nutriosomes: prebiotic delivery systems combining phospholipid, soluble dextrin and curcumin to counteract intestinal oxidative stress and inflammation

1. INTRODUCTION

Starchs are abundant, low-cost, renewable and biodegradable molecules frequently used in food, papermaking, packaging industries, and textiles as well as in medicine, pharmacy and cosmetics. Their indigestible form is often used as a fiber supplement, and they are indispensable constituents of healthy diet, since their daily use promotes beneficial physiological effects by lowering cholesterol, triglycerides, and glucose levels [34,35]. Additionally, exposure to stress, alcohol or drugs diminishes the populations of microorganisms that naturally flourish in human intestine, and some fibers can exert a prebiotic action by nourishing and replenishing the healthy flora of the digestive tract [36]. The dietary use of prebiotics can prevent diarrhoea, intestinal irritation, ulcer, and colon cancer. Dextrins are low-molecular weight carbohydrates derived from dextrose and obtained from the hydrolysis of starch. The indigestible form of dextrin is often used as a fiber supplement. Nutriose® is an indigestible dextrin fiber (85%), sugar free, off-taste, water soluble, and stable at low pH. It possesses α1-2, α1-3 linkages that cannot be hydrolysed in the small intestine of mammals, but are fermented by intestinal bacteria [37]. Previous studies demonstrated that a daily dose of up to ~90 g of Nutriose® is well tolerated in man and provides beneficial effects on intestinal flora [38]. Moreover, its use in pharmaceutical formulations can offer protection against colitis, in synergy with a natural flavonoid [39].

Antioxidant flavonoids have been widely used as protective and curative agents in intestinal pathologies, and chronic inflammatory colon disorders [40–42]. Their loading in nanoparticulate systems plays an important role in maximizing their efficacy, thanks to enhanced bioavailability and targeted delivery [39,43].

In the present work, a soluble dextrin (Nutriose® FM06) and a potent natural antioxidant, curcumin, were combined with phospholipids to obtain promising oral delivery systems, named nutriosomes. The novelty and the advances of this study include the development of nutriosomes by a smart and green method: they self-assembled predominantly in unilamellar nanovesicles where the dextrin is solubilized in the aqueous compartment within the vesicles, as well as in the inter-vesicle medium, thus playing a double role of payload and vesicle structuring agent. Moreover, the simultaneous nanoincorporation of prebiotic Nutriose® and antioxidant curcumin provide a converging efficacy on intestinal health. Nutriosomes were further modified by adding hydroxypropylmetylcellulose, which is expected to improve their stability [34]. Nutriosomes were deeply characterized, and their *in vitro* and *in vivo* performances were studied. In particular, the *in vitro* resistance of vesicles to pH and ionic strength was evaluated, along with their internalization by intestinal cells, and their protective effect against oxidative stress. Moreover, the chemical stability of curcumin and its release from the vesicle formulations were investigated. The *in vivo* biodistribution of vesicles after oral administration and the efficacy against chemically-induced colitis were also evaluated.

2. MATERIALS AND METHODS

Materials

Soy phosphatidylcholine (Phospholipon® 90G, P90G) was purchased from Lipoid GmbH (Ludwigshafen, Germany). Nutriose FM06®, a soluble dextrin from maize, was kindly provided by Roquette (Lestrem, France). Curcumin, hydroxypropylmetylcellulose (HPMC), 2,4,6-trinitrobenzenesulfonic acid (TNBS), and other reagents were purchased from Sigma-Aldrich (Milan, Italy). All the products and solvents were of analytical grade.

Sample preparation

To prepare nutriosomes, P90G (320 mg), curcumin (20 mg), Nutriose® (100 mg), hydroxypropylmetylcellulose (2 mg, when appropriate) were weighed in a glass flask, hydrated with 2 ml of bidistilled water and left swelling for 5 h. Then, the suspension was sonicated (2 sec on and 2 sec off, 30 cycles; 13 microns of probe amplitude) with a high intensity ultrasonic disintegrator (Soniprep 150, MSE Crowley, London, UK). Liposomes without Nutriose® were used as a reference. The exact sample composition is reported in Table 1. The samples were purified from non-incorporated curcumin by dialysis against water using Spectra/Por® membranes (12-14 kDa MW cut-off; Spectrum Laboratories Inc., DG Breda, The Netherlands).

Vesicle characterization

Vesicle formation and morphology were assessed by cryogenic transmission electron microscopy (cryo-TEM). A thin aqueous film was formed by placing a drop of each sample on a glow-discharged holey carbon grid and then blotting it with filter paper. The resulting thin films were vitrified by plunging the grid (kept at 100% humidity and room temperature) into ethane maintained at its melting point, using a Vitrobot (FEI Company, Eindhoven, The Netherlands). The vitreous films were transferred to a Tecnai F20 TEM (FEI Company) using a Gatan cryotransfer (Gatan, Pleasanton, CA), and the samples were observed in a low-dose mode. Images were acquired at 200 kV at a temperature between -170/-175 °C by using low-dose imaging conditions not exceeding 20 $e^{-}/Å^{2}$, with a CCD Eagle camera (FEI Company).

The intensity-weighted mean diameter and polydispersity index (PI; a dimensionless measure of the broadness of the size distribution) were determined by Photon Correlation Spectroscopy using a Zetasizer nano-ZS (Malvern Instruments, Worcestershire, UK), which analyzes the fluctuations in intensity of the light backscattered by particles in dispersion. Zeta potential was estimated using the Zetasizer nano-ZS by means of the M3-PALS (Mixed Mode Measurement-Phase Analysis Light Scattering) technique, which measures the particle electrophoretic mobility.

Curcumin content was quantified after disruption of the vesicles with methanol (1:1000), by using a HPLC chromatograph (Thermo Scientific, Madrid, Spain) equipped with a C18 Novapak column (Waters, Madrid, Spain). The mobile phase consisted of a mixture of acetonitrile/water/acetic acid (50:49:1), delivered at a flow rate of 1 ml/min, and detection was performed at 425 nm. The entrapment efficiency (EE%) was calculated and expressed as the percentage of curcumin post-dialysis *vs.* pre-dialysis.

Vesicle stability

The vesicle dispersions were stored at 25 °C for 90 days, and their mean diameter, polydispersity index and zeta potential were measured at different time points. In parallel, the dispersions were freeze-dried, stored at 25 °C in air or under vacuum, and rehydrated at scheduled time periods to measure the mean diameter, polydispersity index and zeta potential.

Vesicle behaviour at gastrointestinal pHs

The vesicles (1 ml) were diluted with 9 ml of an acidic solution (pH 2) or a neutral solution (pH 7) containing sodium chloride (0.3 M), transferred into the basket of a dissolution rotating apparatus (US Pharmacopeia), thermostated at ~37°C and maintained for 2 h at pH 2, or for 6 h at pH 7. The mean diameter, polydispersity index and zeta potential of the vesicles were measured immediately after the dilution and at the end of the experiments.

Small-Angle X-ray Scattering (SAXS)

SAXS measurements were performed at the BL11-NCD (Non-Crystalline Diffraction) beamline at ALBA synchrotron facility (Cerdanyola del Vallès, Barcelona, Spain). The X-ray beam had a flux of 10^{12} photons/sec, with an energy of 10 keV and wavelength of 0.124 nm. The usable q range was 0.09-4.77 nm^{-1}. The samples were loaded in a flow through glass capillary mounted on an Anton Paar (Graz, Austria) KPR Peltier sample stage, which kept the temperature at 25 ºC. The ensemble was fixed to a motorized sample-stage, which allowed the sample to be aligned and oriented in the

beam. Bidimensional X-ray scattering patterns were acquired using an ADSC Quantum 210r CCD detector. Exposure time per frame was 5 sec. The images were radially averaged and summed. Two series of diffraction patterns were obtained from the same capillary with a separation of 500 μm to check for reproducibility and possible radiation damage (which was not detected throughout the experiments). SAXS patterns were analyzed using a home-made fitting procedure based on a Gaussian description of the bilayers. Since symmetric bilayers did not give an accurate description of the spectra, the possibility of having different electronic density in the polar head region of one and the other side of the bilayer was introduced [45]. The fitting model previously described by Caddeo et al. [45], was employed with a slight modification of the equation used to describe the polar heads represented by a symmetric Gaussian function, using $\Delta\rho_{h1}$ and $\Delta\rho_{h2}$ instead of an additional Gaussian (Eq. 1):

$$G_{h1}(z) = \frac{1}{\sqrt{2\pi}}\Delta\rho_{h1}\exp\left(-\frac{(z-z_{h1})^2}{\sigma_{h1}^2}\right) + \frac{1}{\sqrt{2\pi}}\Delta\rho_{h2}\exp\left(-\frac{(z+z_{h1})^2}{\sigma_{h1}^2}\right)$$

***In vitro* bioactivity of curcumin formulations against oxidative stress**

Caco-2 cells were grown as monolayer in 75 cm^2 flasks, at 37 °C in humidified atmosphere of 5% CO_2 in air. Dulbecco's Modified Eagle Medium high glucose, containing L-glutamine, supplemented with 10% foetal bovine serum, 1% penicillin/streptomycin and 1% fungizone, was used as growth medium. Cells were seeded into 96-well plates at a density of 7.5×10^3 cells/well. After 24 h of incubation, cells were exposed to hydrogen peroxide (1:30000 dilution) for 4 h, in the presence or absence of curcumin in aqueous dispersion or loaded in vesicles (final concentration of curcumin 20 μg/ml). Cells treated with hydrogen peroxide-only were used as a positive control. After 4 h of incubation, the cells were washed with fresh medium, and their viability was determined by the MTT [3(4,5-dimethylthiazolyl-2)-2, 5-diphenyltetrazolium bromide] colorimetric assay, by adding 100 μl of MTT reagent (0.5 mg/ml in PBS) to each well. After 3 h, the formed formazan crystals were dissolved in dimethyl sulfoxide, and the concentration was

spectrophotometrically quantified at 570 nm with a microplate reader (Synergy 4, Reader BioTek Instruments, AHSI S.p.A, Bernareggio, Italy). The results are reported as the percentage of untreated cells (100% viability).

In vitro curcumin stability and release

The stability of curcumin loaded in vesicles was assessed by monitoring the chromatographic profile and the concentration of the polyphenol over 8 h of incubation in cell medium under constant stirring at 37 °C, by HPLC (see Vesicle characterization section).

The release of curcumin from the vesicles was measured by diluting the formulations (2 ml) with cell medium (2 ml), and keeping the dispersions under stirring for 8 h at 37 °C. At regular time intervals (2, 4, 6 and 8 h), samples were centrifuged at 10000 rpm for 5 min at 0 °C. After centrifugation, the formation of three strata was observed: the superior one was yellow transparent and contained the smaller vesicles, the intermediate one was gel-like and yellowish and contained the larger vesicles, and the inferior one was intensely coloured in yellow/orange and contained free curcumin. The two vesicle strata were recovered and the initial volume (4 ml) was restored with fresh medium to continue the release study, while the pellet was solubilized in methanol to quantify curcumin by HPLC.

In vitro cell uptake of vesicles

Caco-2 cells were grown as monolayer in poly-L-Lysine coated 8-well μ-slide (Ibidi GmbH, Martinsried, Germany) and incubated with the vesicles labelled with 1,2-dioleoyl-sn-glycero-3-phosphoethanolamine-N-(lissamine rhodamine B sulfonyl (Rho-PE; Avanti Polar Lipids, Alabama), and 5(6)-carboxyfluorescein (CF, Sigma-Aldrich, Milan, Italy). The uptake of the vesicles was investigated in living cells, at 1, 2 and 4 h, by confocal laser scanning microscopy (CLSM) using a FluoView FV1000 confocal microscope (Olympus, Barcelona, Spain). Pictures were taken in z-stacks using a 60× objective.

In vivo studies

In vivo studies adhered to the principles of laboratory animal care and use, and were performed in accordance with the European Union regulations for the handling and use of laboratory animals and the protocols were approved by the Institutional Animal Care and Use Committee of the University of Valencia (code 2016/VSC/PEA/00159 type 2). Male Wistar rats, aged 8-12 weeks and weighing 230-250 g, were housed in air-conditioned rooms at 22±3°C, 55±5% humidity, 12 h light/dark cycles, with free access to water and chow.

Intestinal biodistribution of hydrophilic macromolecules

Phycocyanin, a macromolecular, hydrophilic, fluorescent marker, was used to label the vesicles and possibly predict the distribution of Nutriose®[46]. The labelled vesicles or the phycocyanin solution (2 ml) were intragastrically administered to healthy rats by gavage (n=4 per group). At 3, 5 and 7 h, rats were sacrificed, the intestines removed, slightly stretched and carefully spread on a dissecting board, and observed by using the In-Vivo FX PRO Imaging System (Bruker BioSpin, USA). Phycocyanin biodistribution was observed (excitation at 640 nm and emission at 680 nm), while curcumin fluorescence overlapped with the spectrum of the intestinal lumen content.

Intestinal biodistribution of curcumin

Curcumin dispersion or curcumin loaded vesicles (2 ml) were intragastrically administered to healthy rats by gavage (n=4 per group). After 3 h, the rats were sacrificed, and liver, kidneys and intestines were excised. The intestines were emptied and divided in segments: duodenum, jejunum, cecum and colon, slightly stretched and carefully spread on a dissecting board. Liver, kidneys, and intestine specimens were soaked in acetonitrile:water (70:30), homogenized and centrifuged at 12500 rpm for 10 min. The amount of curcumin was quantified by HPLC (see Vesicle characterization section). Results were expressed as the ratio of the amount of curcumin in the harvested organ *vs.* the amount of curcumin administered.

Pharmacokinetics of curcumin

Twenty-four hours before curcumin administration, animals were subjected to jugular vein cannulation, and after surgery, they were allowed to recover from the anesthesia. 3 ml of curcumin dispersion (10 and 20 mg/ml) or curcumin loaded vesicles (10 mg/ml) were intragastrically administered to healthy rats by gavage (n=5 per group). After administration, blood samples (0.2 ml) were withdrawn into heparinized syringes at scheduled time points, up to 8 h. Each blood sample was deproteinized with acetonitrile and centrifuged at 3000 rpm for 5 min, and the plasma was stored at -20ºC until assayed for curcumin content by HPLC. The chromatographic analyses were performed in a Perkin Elmer® HPLC Series 200 equipped with a binary pump, an auto-sample and a fluorescence detector. Identification and quantification of curcumin were performed in a Teknokroma® Brisa "LC2" C18 column (5.0 µm, 150 × 4.6 mm). Curcumin was eluted isocratically at a flow rate of 1 ml/min using 20 mM acetate buffer pH 3.0 and methanol (40:60, v/v) as a mobile phase, and 50 µl for the injection volume. Excitation and emission wavelengths of elute fluorescence were optimized for measurement at 420 and 530 nm, respectively.

The pharmacokinetic parameters were calculate using a non-compartmental analysis by Phoenix WinNonlin®. The maximum observed plasma concentration (C_{max}) and the time taken to reach it (t_{max}) were obtained from the curve plotting curcumin concentration *vs.* time. The area under each drug concentration time curve (AUC, ng/ml h) to the last data point was calculated by the linear trapezoidal rule and extrapolated to time infinity by the addition of C_{Last}/Ke, where C_{Last} is the concentration of the last measured plasma sample.

Efficacy of curcumin against colitis

Chronic inflammation in rat colon was chemically induced as previously described [39,47], with slight modifications. Rats (n=4 per group) were anesthetized with isoflurane, and TNBS (0.13 M) dissolved in ethanol/water (50:50) was instilled (0.5 ml) into the colon lumen (day 0). Healthy animals were the negative control; animals with TNBS-induced colitis treated with saline were the

positive control; the other groups consisted of animals with colitis receiving curcumin dispersion or curcumin liposomes, nutriosomes or HPMC-nutriosomes (2 ml) by oral gavage daily for 3 days, when inflammation was most intense (days 3, 4 and 5 after TNBS rectal administration).

On day 9, the rats were euthanized with an overdose of sodium pentobarbital (Dolethal®, Vetoquinol, UK), the abdomen was cut open, and the distal colon was removed. The extent and severity of colitis was evaluated by visual inspection of the excised colon, along with the measurement of myeloperoxidase activity (MPO). MPO was used as an index of inflammation and was measured according to an established method [39,47]. Briefly, each colon specimen was soaked in 750 μl of hexadecyltrimethylammonium bromide buffer (0.5% in 80 mM phosphate buffer pH 5.4) and homogenized. The homogenate was centrifuged (Heraeus Fresco 17 Centrifuge, Thermo Electron Corporation, Spain) at -1°C and 1000 rpm for 15 min. The supernatant was incubated with hydrogen peroxide and tetramethylbenzidine. The reaction was stopped with 2 N H_2SO_4, and the absorbance was measured spectrophotometrically at 450 nm.

Statistical analysis of data

Results are expressed as the mean±standard deviation. Analysis of variance (ANOVA test) was performed to assess the differences among groups using the IBM SPSS statistics 20.0 for Windows. Post hoc testing (p=0.05) of multiple comparisons was performed by the Scheffe or Dunnet tests.

3. RESULTS

Vesicle characterization

Nutriosomes, HPMC-nutriosomes and liposomes were easily fabricated in a one-step procedure, without the use of organic solvents or energetic and dissipative procedures, by keeping the phospholipid and the other components in water, and by sonicating the dispersion to form lamellar vesicles and adjust their size and lamellarity. The sample composition is reported in Table 1.

Table 1. Composition of curcumin loaded liposomes, nutriosomes and HPMC-nutriosomes.

	P90G (mg/ml)	**Curcumin (mg/ml)**	**Nutriose (mg/ml)**	**HPMC (mg/ml)**
Liposomes	160	10	0	0
Nutriosomes	160	10	50	0
HPMC-nutriosomes	160	10	50	1

The actual formation of the vesicles and their morphology were confirmed by cryo-TEM observation. The images of liposomes displayed spherical and mostly unilamellar vesicles, with a few multilamellar vesicles (Figure 1A). Nutriosomes were spherical in shape, and both multilamellar, multicompartment structures and unilamellar vesicles were observed (Figure 1B). HPMC-nutriosomes were basically spherical and unilamellar (Figure 1C).

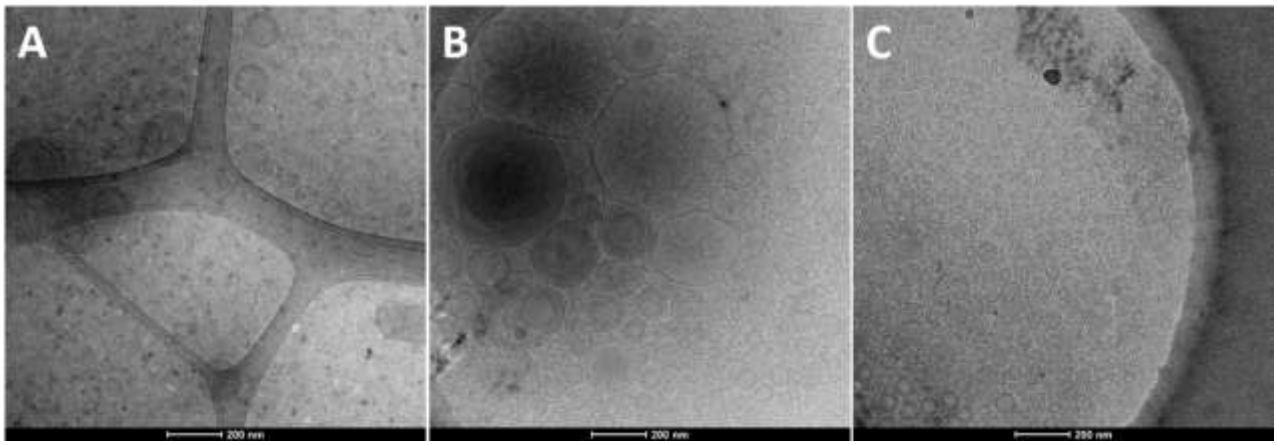

Figure 1. Representative cryo-TEM images of curcumin loaded liposomes (A), nutriosomes (B) and HPMC-nutriosomes (C).

The mean diameter of empty liposomes was ~107 nm, and the addition of curcumin led to a significant increase in size up to ~181 nm ($p<0.01$) and zeta potential from -12 to -37 mV ($p<0.01$), which indicate a localization of curcumin not only within the bilayer, but also onto the bilayer surface (Table 2) [48,49].

Table 2. Mean diameter (MD), polydispersity index (PI), zeta potential (ZP) and entrapment efficiency (EE) of empty and curcumin loaded liposomes, nutriosomes and HPMC-nutriosomes. Mean values (n=6) ± standard deviation are reported. Different symbols (#, *) indicate statistically different values.

	MD (nm)	**PI**	**ZP (mV)**	**EE (%)**
Empty liposomes	107±8	0.35	-12±4	
Empty nutriosomes	127±7	0.24	-13±3	
Empty HPMC-nutriosomes	135±6	0.31	-14±6	
Curcumin liposomes	181±7	0.33	-37±4	#73±6
Curcumin nutriosomes	183±8	0.35	-39±2	*88±7
Curcumin HPMC-nutriosomes	153±8	0.34	-36±7	*91±6

The addition of Nutriose® led to a small increase of the mean diameter of empty nutriosomes in comparison with empty liposomes (from ~107 to ~127 nm, $p<0.05$), while in curcumin loaded nutriosomes the effect of the dextrin was mitigated by the presence of the polyphenol, as liposomes and nutriosomes showed the same mean diameter and zeta potential (~182 nm and ~-38 mV, $p>0.05$ between the two samples). The further addition of HPMC led to a slight increase in size for empty nutriosomes, while a decrease was observed upon incorporation of curcumin (~153 nm, $p<0.05$ *vs.* liposomes and nutriosomes).

The stability of the vesicle dispersions was evaluated during storage at 25°C. After 60 days, the mean diameter of all the samples significantly increased (data not shown). As an alternative, the dispersions were freeze-dried and kept at 25°C in air or under vacuum. The samples were rehydrated every 30 days up to 180 days, and the size, polydispersity index and zeta potential were measured (Figure 2).

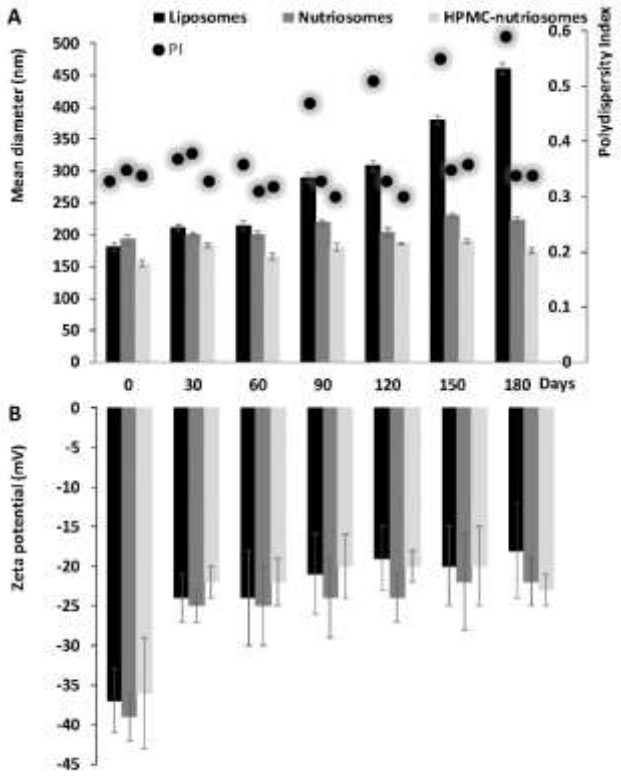

Figure 2. Mean diameter, polydispersity index (PI) and zeta potential of curcumin loaded liposomes, nutriosomes and HPMC-nutriosomes lyophilized, kept under vacuum for 180 days, and rehydrated at different time periods. Bars represent standard deviations (n=3).

The size of liposomes remained almost constant during the first 60 days, then the mean diameter and polydipersity index increased up to ~450 nm and 0.6, respectively. On the contrary, the parameters of both nutriosomes and HPMC-nutriosomes remained constant over the whole storage period, indicating a positive effect of Nutriose® on the vesicle re-formation, probably because the

soluble dextrin acted as a cryo-protector avoiding structural collapse of the vesicles during the dehydration process.

The resistance of the vesicles to pH variations and ionic strength was evaluated by incubating the formulations with appropriate solutions (pH 2 or 7 and 0.3 M NaCl), and monitoring the vesicle size, polydispersity index and zeta potential (Table 3) [39].

Table 3. Mean diameter (MD), polydispersity index (PI), zeta potential (ZP) and entrapment efficiency (EE) of liposomes, nutriosomes and HPMC-nutriosomes diluted and incubated with acidic solution (pH 2) for 2 h or with neutral solution (pH 7) for 6 h, both containing sodium chloride (0.3 M), at 37°C. The measurements were carried out immediately after the dilution (t_{0h}) and after 2 h at pH 2 (t_{2h}) and 6 h at pH 7 (t_{6h}). Mean values ± standard deviation are reported.

	pH	**Time**	**MD (nm)**	**PI**	**ZP (mV)**	**EE (%)**
Liposomes	2	t_{0h}	205±40	0.41	13±3	
		t_{2h}	557±20	0.58	11±2	79±6
Nutriosomes	2	t_{0h}	174±15	0.37	13±4	
		t_{2h}	394±49	0.50	8±5	93±10
HPMC-nutriosomes	2	t_{0h}	199±19	0.40	10±4	
		t_{2h}	224±42	0.49	9±5	89±9
Liposomes	7	t_{0h}	181±20	0.42	0±2	
		t_{6h}	162±5	0.39	-1±2	33±12
Nutriosomes	7	t_{0h}	170±7	0.47	0±2	
		t_{6h}	166±49	0.41	-4±3	49±5
HPMC-nutriosomes	7	t_{0h}	134±21	0.48	-2±5	
		t_{6h}	204±8	0.49	-1±2	56±7

After 2 h at pH 2, the size of liposomes increased up to 557 nm and the polydispersity index up to 0.58, which indicats a partial loss of their structure. On the contrary, the size of nutriosomes was less affected by the acidic pH (394 nm), and even less in the case of HPMC-nutriosomes (224 nm). Under these conditions, the zeta potential of the samples turned to positive values. After 6 h at pH 7, both liposomes and nutriosomes did not undergo marked alterations, while HPMC-nutriosomes increased in size, presumably due to swelling, which follows polymer hydration leading to relaxation of polymer chains and their entanglement to form a viscous gel layer around the vesicles.

SAXS analysis

Empty liposomes showed the typical spectra of multilamellar vesicles (Figure 3A), with a large number of unilamellar (i.e., uncorrelated) structures (20% correlation; Table 4), while curcumin loaded liposomes (phospholipid:curcumin molar ratio 8.6:1) were predominantly unilamellar, with a small population (6%; Table 4) of multilamellar (i.e., correlated) vesicles (Figure 3A).

The multilamellar liposomes, from both spectra, showed similar repetition distance (d, 6.21 and 6.28 nm for empty and curcumin loaded liposomes, respectively; Table 4). Because of the high preponderance of unilamellar vesicles, the parameters associated with the structure (Caillé parameter η, and number of correlated and uncorrelated lamellae N and N_{unc}) have high uncertainty. The main differences in the bilayer structure of empty and curcumin loaded liposomes refer to the width of the head group and methylene gaussians (σ_h and σ_c, respectively; Table 4), which are smaller for curcumin loaded liposomes, as can also be observed in the electron density plots showing more pronounced polar head and methylene gaussians (Figure 3B). This is in contrast with the observations of Hung et al. [16] that observed an increase of both σ_h and σ_C when curcumin was added to dioleoylglycerophosphocholine liposomes. Moreover, Hung et al. detected a reduction in the phosphate peak-to-phosphate peak distance (equivalent to 2 Z_h) of about 0.1 nm for curcumin/lipid molar ratios above 0.02, while we observed a reduction of 0.03 nm at the present

curcumin/lipid molar ratio of 0.13. However, it has to be noted that Hung et al.'s experiments were conducted below complete hydration.

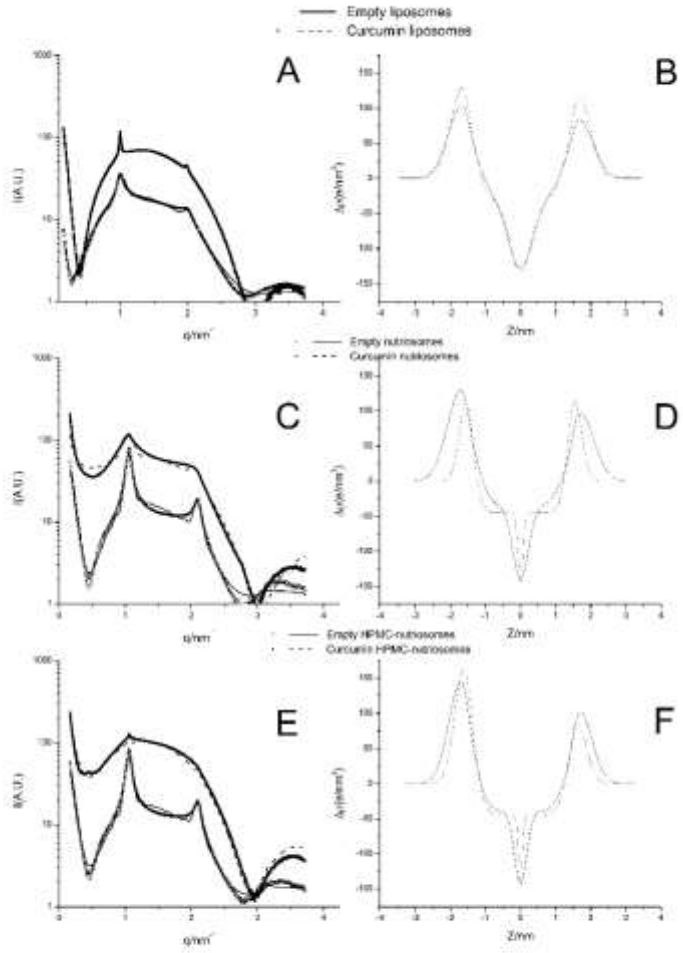

Figure 3. Experimental SAXS intensity (symbols) and fitted model (lines) are shown in the left panel, electron density profiles in the right panel for empty and curcumin loaded liposomes (A-B), nutriosomes (C-D), and HPMC-nutriosomes (E-F).

The electron density of the polar head ($\Delta\rho_h$; Table 4) increased when curcumin was loaded, which might be a consequence of curcumin replacing some of the water molecules that hydrate the polar heads.

The scattering profiles of empty and curcumin loaded nutriosomes were the result of the subtraction of Nutriose® (50 mg/ml) spectrum (Figure 3C). The profile of empty nutriosomes showed the typical peaks of multilamellar vesicles (corresponding to 42% of the sample; Table 4). Nutriose® seems to interact weakly with the bilayer, as demonstrated by the similar spectra of empty liposomes and nutriosomes. This can be explained by the fact that water-soluble Nutriose® is supposedly localized in the aqueous compartments of the vesicles (internal core, interlamellar space, and intervesicle medium). However, the dextrin seems to affect the arrangement of the vesicles, as it increased the lamellarity (from 20 to 42% of multilamellar structures; Table 4) and rigidity observed as a significant reduction of Caillé parameter (η; Table 4) when comparing the results of nutriosomes and liposomes. These effects can be due to the ability of Nutriose® to reduce the interlamellar repulsion due to its solubilization in the aqueous layers where solvent dielectric constant is decreased as a result of the increased number of ionized groups on the interfacial bilayer regions [51,52].

Table 4. Fitting derived parameters obtained from SAXS analyses at 25 °C of empty and curcumin loaded liposomes, nutriosomes and HPMC-nutriosomes. Mean values ± standard deviation are reported.

	Empty liposomes	**Empty nutriosomes**	**Empty HPMC-nutriosomes**	**Curcumin liposomes**	**Curcumin nutriosomes**	**Curcumin HPMC-nutriosomes**
d (nm)	6.21±0.05	5.97±0.05	5.97±0.05	6.28±0.05	6.10±0.05	5.98±0.05
η	0.10±0.04	0.06±0.01	0.07±0.01	0.12±0.05	0.04±0.04	0.05±0.01
N	5.9±2	7.9±1	8.0±1	54±2	3.9±1	15±4
σ_h (nm)	0.39±0.05	0.39±0.05	0.35±0.05	0.33±0.05	0.42±0.02	0.15±0.05
$\Delta_{\rho h1}$ (e/nm^3)	83±5	97±5	102±5	115±5	52±5	89±5
$\Delta_{\rho h2}$ (e/nm^3)	103±5	129±5	146±5	129±5	53±5	168±5
Z_h (nm)	1.67±0.05	1.70±0.05	1.69±0.05	1.66±0.05	1.63±0.05	1.60±0.05
σ_c (nm)	0.35±0.10	0.22±0.10	0.17±0.10	0.29±0.10	0.07±0.10	0.05±0.10
N_{unc}	24±5	11±5	10±5	800±100	5.9±2	650±1000
% correlation	20	42	43	6	29	2

d, repetition distance; η, Caillé parameter; N, number of correlated lamellae; σ_h, polar head Gaussian width with electron density difference to the media, $\Delta_{\rho h1}$ and $\Delta_{\rho h2}$, for each bilayer leaflet; Z_h, position of the polar head Gaussian with respect to the bilayer center; σ_c, methylene groups Gaussian width at the center of the bilayer; N_{unc}, number of uncorrelated lamellae.

A reduction of the lamellar spacing was also observed (d, from 6.21 to 5.97 nm; Table 4), which may be caused by an increase in rigidity of the bilayers. On the other hand, the presence of curcumin reduced the intensity of the peaks, and the bands corresponding to unilamellar vesicle predominate. When comparing the electron density profiles of empty and curcumin loaded nutriosomes, the main finding is the thinning of the bilayer (i.e., decrease in thickness) when curcumin was loaded, due to the dehydration of the polar heads (Figure 3D; σ_H, Table 4). At the same time, the hydrophobic part (Figure 3C; σ_C, Table 4) of the phospholipid became more ordered,

and the dip due to the methylene groups became more distinct, which is probably a consequence of the partial dehydration of the polar heads.

In Figure 3E, the spectra of empty and curcumin loaded HPMC-nutriosomes are reported. As can be deduced by comparing the spectra of HPMC-nutriosomes and nutriosomes, the effect of HPMC on the bilayer structure and ordering is minimal. Again, curcumin reduced notably the number of multilamellar vesicles (from 43 to 2%; Table 4), as only a small signal corresponding to multilamellar structures was still visible. The effect of curcumin was very similar to that observed in curcumin loaded liposomes, which showed a spectrum typical of an entirely unilamellar vesicle system, with a small population (6% and 2% for curcumin liposomes and HPMC-nutriosomes, respectively; Table 4) of significantly multilayered vesicles. This effect can be deduced from the comparison of the number of correlated bilayers and uncorrelated bilayers (N and N_{unc}, respectively; Table 4).

While the asymmetry of the bilayer (as quantified by the difference between $\Delta\rho_{h1}$ and $\Delta\rho_{h2}$) is only marginally affected by the presence of Nutriose®, it seems clear that the presence of HPMC has a strong effect, increasing the electron density difference (Figure 3F). We should remark that a similar effect on the fitting could be obtained by letting the headgroup position to differ, instead of the electron density, because both have a strong cross-correlation and the fits of the HPMC were not optimal.

Summarizing, we can say that the effect of curcumin is dramatic on the SAXS profiles of all the vesicle systems studied, which is not on the bilayer thickness and electron density distribution, but on the lamellarity. At present, the reason behind the strong increase in the presence of uncorrelated lamellae (i.e., unilamellar structures) is not clear. The overall effect of curcumin on the bilayer is an increase in rigidity (decrease of Caillé parameter η) and a reduction of the width of the polar heads (σ_h). On the other hand, the presence of Nutriose® and HPMC increase the dissymmetry of the bilayer, which suggests that they partition preferably to one of the leaflet. Since the model does not

distinguish between the inner and the outer leaflet, we cannot say whether Nutriose® and HPMC are localized/adsorbed in the concave or convex leaflet.

In vitro bioactivity of curcumin formulations against oxidative stress

The ability of curcumin loaded vesicles to neutralize free radicals and protect Caco-2 cells from oxidative stress caused by hydrogen peroxide was demonstrated, as compared to the effect of curcumin dispersion at the same concentration (Figure 4).

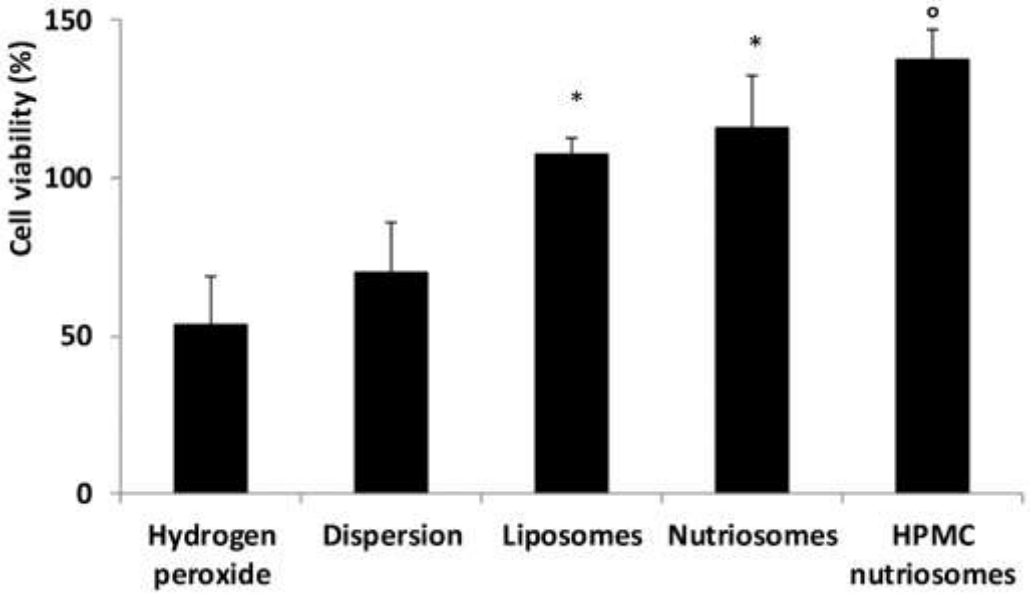

Figure 4. Viability of Caco-2 cells exposed to hydrogen peroxide alone or simultaneously treated with curcumin aqueous dispersion or curcumin loaded liposomes, nutriosomes and HPMC-nutriosomes. Data are reported as mean values ± standard deviation (error bars) of cell viability expressed as the percentage of the negative control (100% viability). *,° different symbols indicate statistically different values ($p<0.05$).

After hydrogen peroxide exposure, cell viability was halved (~50%). It increased slightly when the curcumin dispersion was applied (~70%, $p>0.05$), to a greater extent when using curcumin loaded liposomes and nutriosomes (~110%, $p<0.05$ between liposomes and nutriosomes, and $p<0.01$ *vs.*

hydrogen peroxide-exposed cells), and even more when using HPMC-nutriosomes (~137%, $p<0.01$ *vs*. all the samples). The results highlighted the important role played by the phospholipid vesicles in enhancing the activity of curcumin, and a further improvement provided by HPMC.

In vitro curcumin stability and release

The chromatographic profiles of curcumin did not show significant variations after incubation in cell medium for 8 h, and the concentration of curcumin did not decrease. This demonstrates that no degradation occurred, thus proving the stability of the polyphenol under the experimental conditions tested (Figure 5 A and B) [53].

The amount of curcumin released from liposomes reached a maximum at 2 h (~80%), and remained constant up to 8 h. On the contrary, the release of curcumin from nutriosomes and HPMC-nutriosomes was lower at 2 and 4 h (~32 and 58%, respectively), and reached 68% at 8 h (Figure 5 c).

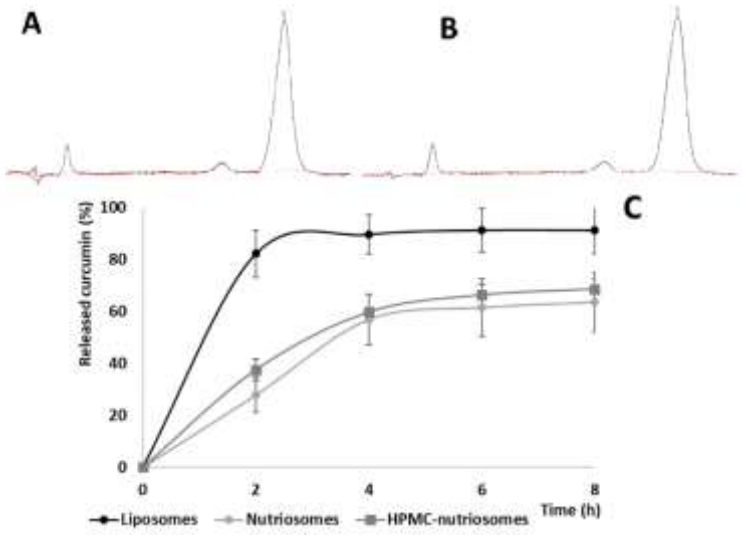

Figure 5. Representative chromatograms of curcumin before (A) and after 8 h of incubation (B) of curcumin liposomes, nutriosomes and HPMC-nutriosomes in cell medium.

Release profiles of curcumin from liposomes, nutriosomes and HPMC-nutriosomes (C) over 8 h in cell medium.

In vitro cell uptake

The uptake of liposomes, nutriosomes and HPMC-nutriosomes by Caco-2 cells was evaluated after 1, 2 and 4 h of incubation with the vesicles labelled with Rho-PE, as a lipid marker (red fluorescence), and CF, as a hydrophilic marker (green fluorescence) (Figure 6). The images of cells incubated with liposomes, at 1, 2 and 4 h disclosed a non-time dependent accumulation of Rho-PE in the perinuclear area, while no localisation of CF within the cells was observed, as it was confined to the external medium. This may indicate that a rupture of liposomes occurred during the internalization process. The images of the cells treated with labelled nutriosomes showed a different behaviour: Rho-PE was localized in the perinuclear area, CF was mainly accumulated in the cytoplasm, and a yellow fluorescence was also observed in the peripheral area of the cytoplasm, which indicates the co-localization of the two probes presumably internalized in intact vesicles. The cells incubated with HPMC-nutriosomes showed an even more evident co-localization of the probes. The yellow fluorescence was similar to that observed for nutriosomes after 1 h of incubation, while it was more intense at 2 and 4 h, which indicates a massive internalization of vesicles and aggregation in the peripheral area of the cytoplasm. The increased uptake of HPMC-nutriosomes is probably related to the presence of the polymer, which may favour the interaction between cells and vesicles.

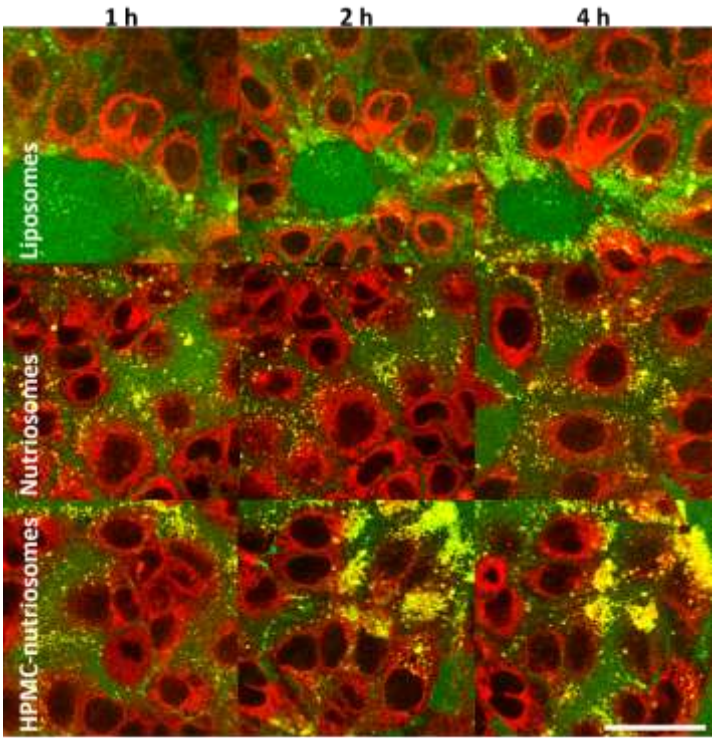

Figure 6. CLSM images of Caco-2 cells exposed to liposomes, nutriosomes and HPMC-nutriosomes labelled with Rho-PE (red) and CF (green) for 1, 2 and 4 h. The bar corresponds to 50 μm.

In vivo biodistribution of hydrophilic macromolecules in the gastrointestinal tract

To evaluate the gastrointestinal transit of the formulations and to establish their ability to facilitate dextrin and curcumin delivery *in vivo*, the vesicles were labelled with phycocyanin, which is a water-soluble, fluorescent macromolecule [54]. The labelled vesicles loading curcumin were administered to healthy rats, and their biodistribution in the gastrointestinal tract was monitored as a function of time by using the In Vivo FX PRO Imaging System, which allowed the precise localization of the markers. An aqueous dispersion of phycocyanin and curcumin was also administered and used as a reference. The fluorescence of phycocyanin was visualized in blue, while the fluorescence of curcumin overlapped with the spectrum of the intestinal lumen content (Figure 7). When the phycocyanin solution was administered, the fluorescence decreased over time:

after 3-5 h, the fluorescence was moderate and restricted to the final part of the intestine, mostly jejunum and slightly in the cecum and colon, while it disappeared after 7 h. Liposomes provided a more widespread and persistent fluorescence in comparison with the solution: after 3-5 h, the signal was more evident in duodenum and jejunum, and after 7 h, a weak signal was visible also in cecum and colon.

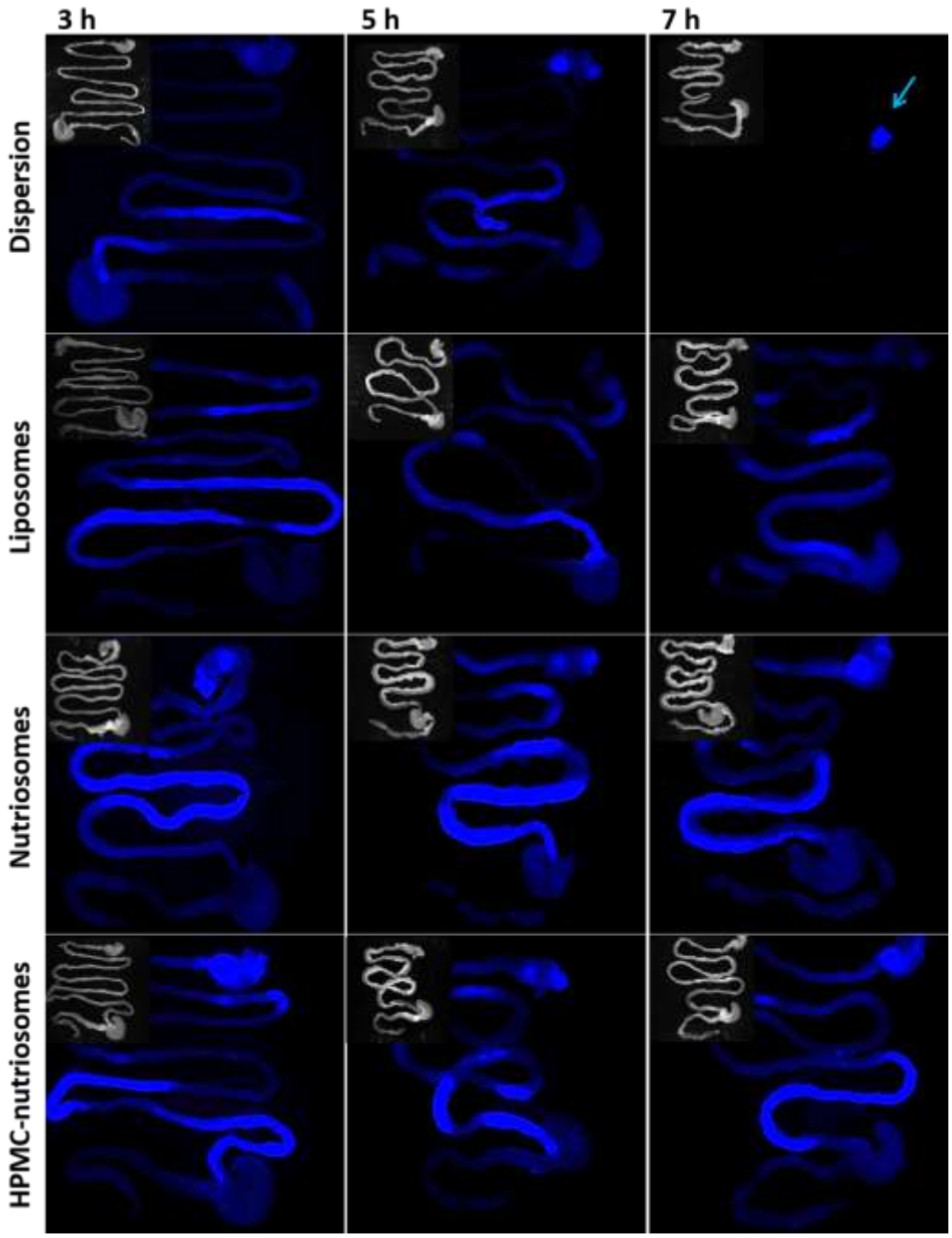

Figure 7. Fluorescence images of the gastrointestinal tract excised from healthy rats treated with a dispersion of phycocyanin and curcumin or phycocyanin-labelled curcumin-loaded liposomes, nutriosomes and HPMC-nutriosomes.

After nutriosome administration, the most intense fluorescence was observed: after 3 h, it was diffused in the stomach, duodenum and upper part of jejunum; after 5 h, it shifted in the whole

jejunum and slightly in the cecum; after 7 h, it was detected in the final part of jejunum and slightly in cecum and colon. After HPMC-nutriosome administration, the florescence distribution was similar to that observed for nutriosomes, but less intense and extensive. Hence, all the vesicles enhanced the fluorescence biodistribution and intensity with respect to that provided by the solution, and especially nutriosomes were able to prolong and extend the distribution of the macromolecule in the whole intestine, even in the colon.

In vivo biodistribution of curcumin in the intestines

The biodistribution of curcumin in the different parts of the intestine, 3 h after administration, was assessed by HPLC quantification (Figure 8).

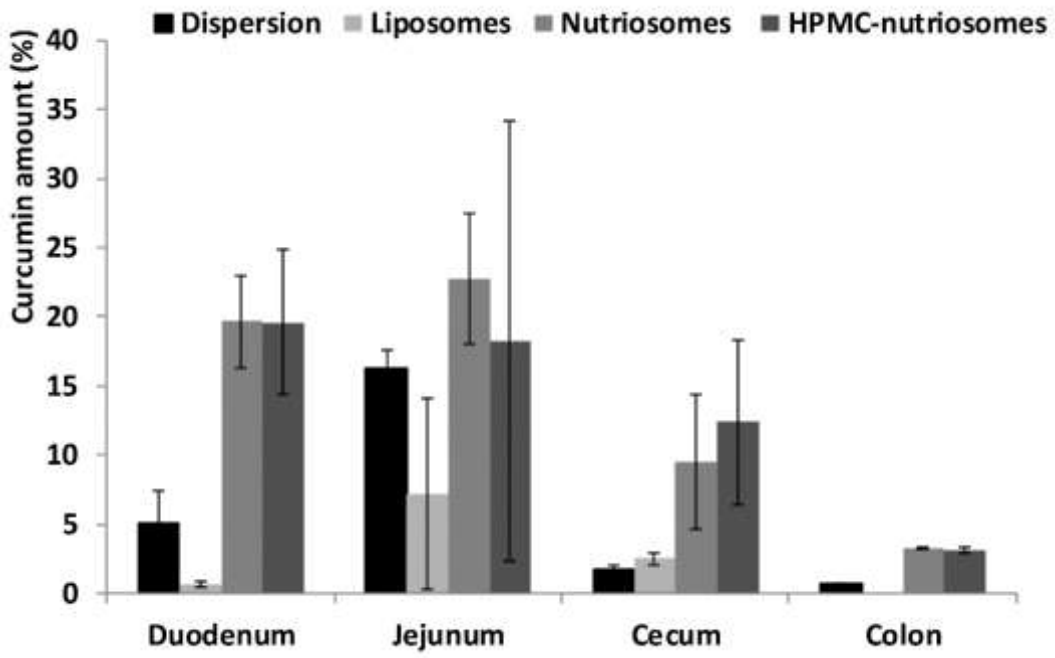

Figure 8. Amount (%) of curcumin found in the different segments of the gastrointestinal tract, 3 h after its administration in aqueous dispersion or in liposomes, nutriosomes and HPMC-nutriosomes. Data are reported as mean values ± standard deviation (error bars).

The dispersion provided a higher accumulation of curcumin in the duodenum (~5%) and jejunum (~16%), and much lower in cecum and colon (~1%). Liposomes allowed a high accumulation in the jejunum (~7%) and cecum (~3%), and less in the other segments (<1%). The accumulation obtained after administration of nutriosomes and HPMC-nutriosomes was similar in the duodenum and jejunum (~20%), while it was higher in the cecum (~12%) and colon (~3%). In agreement with the biodistribution of the hydrophilic marker, this study confirmed the superior ability of nutriosomes and HPMC-nutriosomes to facilitate the local accumulation of curcumin in the intestines. *In vivo* biodistribution results showed that the amount of curcumin found in liver and kidneys was negligible (data not shown).

Pharmacokinetics of curcumin

The pharmacokinetic studies showed the effect of the nanoincorporation on curcumin plasma concentration. Curcumin levels in blood were determined at 10 different time points up to 8 h after a single dose of dispersion or vesicle formulations administered in rats orally (Figure 9).

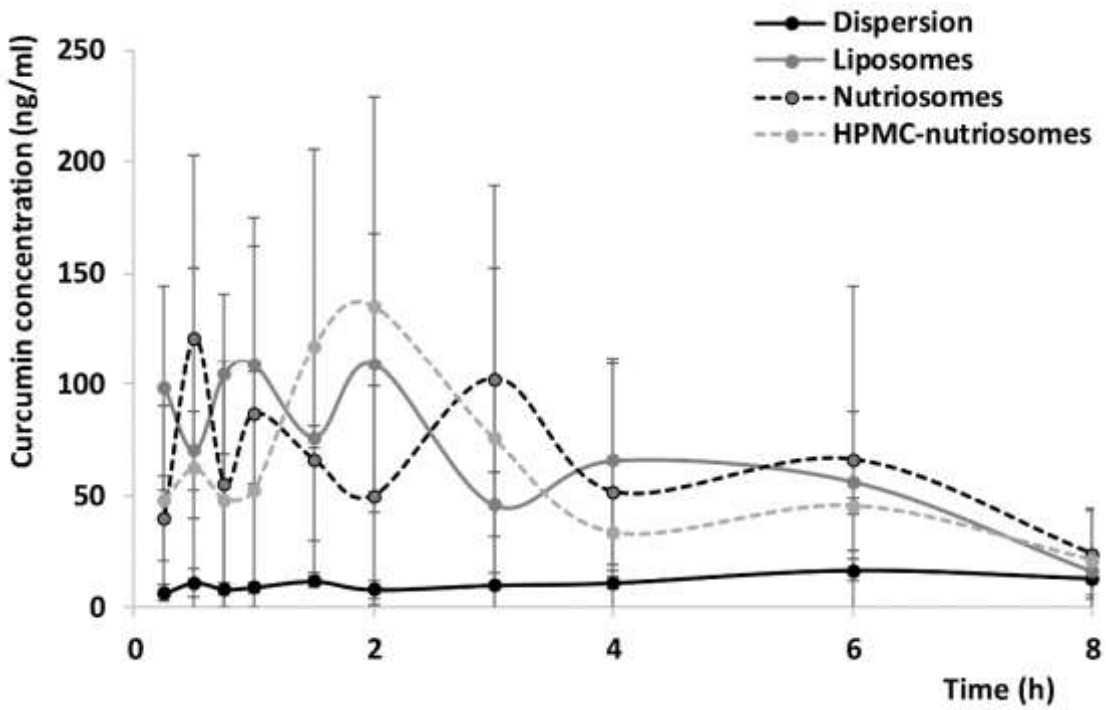

Figure 9. Curcumin plasma concentration over 8 h after a single-dose administration of an aqueous dispersion or liposomes, nutriosomes and HPMC-nutriosomes. Data are reported as mean values ± standard deviation (error bars).

The plasma concentration of curcumin was not detectable when administering 30 mg of the polyphenol in aqueous dispersion, and a double amount (60 mg) was necessary to allow quantification. The plots of plasma concentration *vs*. time displayed a flat and low pharmacokinetic profile for the dispersion, as compared to fluctuating and higher profiles observed for all the vesicle formulations. C_{max}/D and AUC/D were more than 10-, 7.25- and 10.44-fold higher when liposomes, nutriosomes or HPMC-nutriosomes were used, in comparison with the curcumin dispersion. T_{max} results should be interpreted with caution, since the measurement of the curcumin plasma concentration, when the dispersion was administered, did not show a C_{max} as clear and high as that observed when using the vesicle formulations (Figure 9). This demonstrates the carrier capabilities of nutriosomes, which facilitated not only the curcumin local accumulation in the whole intestine, but also the passage of the polyphenol through the intestinal mucosa towards the systemic circulation, providing a maximum concentration 12-15-fold higher (C_{max}/D), and an overall exposure up to 10-fold higher (AUC_{last}/D) than that of the dispersion using half of the dose.

***In vivo* efficacy of curcumin against colitis**

Colitis was induced in rats by intracolonic application of TNBS, and the therapeutic efficacy of curcumin was assessed as a function of the incorporation in the investigated nutriosomes and liposomes. The tissue damage was macroscopically evaluated by visual inspection of the internal and external walls of the colon (Figure 10). The colon of healthy rats was intact and pink-coloured, with a constant width for the entire length. The colon from TNBS rats treated with saline (positive control) showed thickening, ulcerated mucosal lesions, and oedematous inflammation, which caused strong dilatation. Similar features were observed when the curcumin aqueous dispersion was administered. On the contrary, the colon of the TNBS rats treated with the vesicle formulations

were very similar to those of healthy controls, in diameter and colour, especially those treated with nutriosomes, while a reduction in length and small necrotic areas were observed in the animals treated with liposomes and HPMC-nutriosomes.

The colonic damage induced by TNBS was associated with an increase in MPO activity in comparison with healthy controls, indicative of neutrophil infiltration in the inflamed tissue.

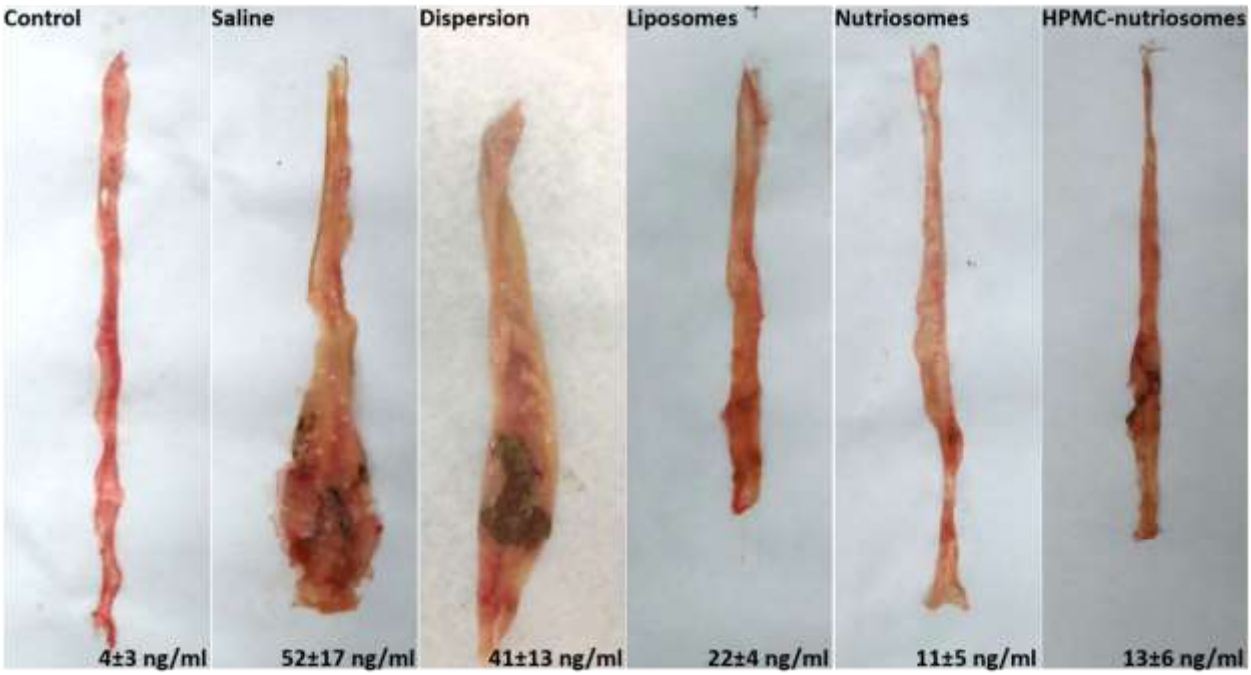

Figure 10. Macroscopic appearance of colon tissue from healthy or colitic rats treated with a curcumin aqueous dispersion or liposomes, nutriosomes and HPMC-nutriosomes. MPO values are reported in ng/ml.

The MPO activity increased significantly in TNBS rats (from 4 to 52 ng/ml; Figure 10), and it was slightly mitigated by the curcumin dispersion. On the other hand, the administration of curcumin loaded vesicles resulted in a marked reduction of MPO activity, especially using nutriosomes and HPMC-nutriosomes (~12 ng/ml; Figure 10), even if the values were not statistically different ($p>0.05$) from that found for liposome-treated animals. The results indicate that liposomes potentiate the ability of curcumin to inhibit MPO, which could not be further extended by

nutriosomes and HPMC-nutriosomes, despite the higher bioavailability of the polyphenol they provide.

4. DISCUSSION

Environmental pollution, modern food and beverages contain additives that can cause oxidative stress in human intestine. The cellular antioxidants are not able to neutralize the overproduced reactive oxygen species (ROS), which results in chronic bowel inflammation and systemic oxidative stress, frequently correlated with carcinogenesis [21].

The findings of the present work confirm that the combination of phospholipid, prebiotic dextrin and antioxidant curcumin in a novel phospholipid vesicle formulation, namely nutriosomes, represents a promising approach to prevent and counteract the above physio-pathological conditions. Moreover, nutriosomes were prepared without the use of organic solvents, by means of a one-step, easy and scalable procedure.

Cryo-TEM and SAXS studies displayed that nutriosomes assembled in unilamellar and multilamellar, multicompartment vesicles, stabilized by the presence of Nutriose® in the inter-lamellar and inter-vesicle medium. The presence of curcumin reduced notably the number of multilamellar vesicles. Additionally, HPMC reduced the vesicle lamellarity producing almost unilamellar-only structures, probably due to the polymer adsorption onto the bilayer surface. The soluble dextrin played an important role as a cryo-protector, avoiding vesicle collapse during the lyophilization process: both nutriosomes and HPMC-nutriosomes, when freeze-dried and stored under vacuum up to 180 days, could be easily re-formed by rehydration, basically preserving their size and structure. The high phospholipid concentration (160 mg/ml) used to prepare the vesicles ensured an acceptable resistance of liposomes to high ionic strength and pH changes encountered in the gastrointestinal environment. The additional presence of Nutriose® improved the resistance of nutriosomes, and HPMC further protected the vesicles, presumably thanks to the formation of a

polymer layer around the surface of the vesicles. It seems reasonable to presume that the incorporation of curcumin in the vesicles prevented direct contact of the polyphenol with the gastro-intestinal media and its degradation.

When the formulations reach the intestines, intact vesicles could enhance the ability of curcumin to neutralize reactive oxygen species associated to oxidative injury in cells [56–58]. The protective effect against hydrogen peroxide-induced oxidative stress in Caco-2 cells, which were used as intestinal cell model because they grow as monolayer and express several morphological and biochemical characteristic of the small intestine enterocytes [59], was evaluated using curcumin in aqueous dispersion or loaded in vesicles. The highest survival of stressed cells was obtained when nutriosomes and mostly HPMC-nutriosomes were used, while the curcumin dispersion was not able to counteract the oxidative effect of hydrogen peroxide. The results confirmed the great ability of nutriosomes to interact with cells and promote the local antioxidant effect of the polyphenol. Its efficacy was further improved by HPMC-nutriosomes, possibly due to the more extensive cell internalisation (Figure 6). Moreover, other factors could contribute to potentiate the curcumin efficacy using HPMC-nutriosomes, such as increased stability, bioavailability, and release rate, which was slower as compared to liposomes (Figure 5).

Nutriosomes exhibited large affinity and distribution towards the epithelial mucosal surface of the intestine, improving to a large extent the local accumulation of both curcumin and water-soluble, macromolecular phycocyanin, used to simulate the fate of Nutriose®, with respect to a dispersion of the polyphenol and phycocyanin, and liposomes.

Previous pharmacokinetic studies on curcumin reported a low intestinal absorption after oral administration, resulting in poor systemic bioavailability and rapid clearance from the body [60–63]. To overcome these problems, several curcumin nanoformulations have been developed and tested [64,65]. Maiti et al. reported the formation of a curcumin complex with phospholipids capable of enhancing its therapeutic efficacy, which was related to better absorption and

bioavailability of the molecule [32]. In this work, curcumin incorporated in liposomes, nutriosomes, and HPMC-nutriosomes showed higher systemic bioavailability (7.44-10.44 fold) in plasma than that provided by the dispersion upon oral administration. Additionally, the vesicles promoted the distribution of curcumin in the intestinal membrane to a greater extent than the free polyphenol in dispersion. Hence, the vesicles could modify the pharmacokinetics and biodistribution of the incorporated curcumin. A similar enhanced effect was previously found by other authors, and might be attributed to an improved diffusion of particles through the mucus, and a higher interaction with the epithelial walls due to the adhesive properties of nanocarriers [66-68].

In addition, the degree of inflammation and tissue injury caused by TNBS was substantially reduced in rats treated with the vesicle formulations, as demonstrated by the reduction of inflammation biomarkers in comparison with the curcumin dispersion.

5. CONCLUSIONS

In the present study, nutriosomes were successfully developed by combining phospholipids at high concentration, a prebiotic dextrin, an antioxidant polyphenol, and possibly a polymer, by using a simple, organic solvent-free, reproducible method. Nutriosomes were proposed as an oral formulation for the protection of intestine, thanks to the combined activity of Nutriose® and curcumin. Physico-chemical investigations demonstrated that the association of the dextrin and the polyphenol in phospholipid vesicles was crucial for vesicle features and stability. Moreover, the results obtained *in vivo* supported the hypothesis that nutriosomes enhanced the accumulation of both the dextrin and curcumin in the different segments of the intestine. The systemic bioavailability of curcumin was also increased after oral administration of the vesicle formulations. Additionally, chemically-induced colonic damage was reduced by the vesicles, in particular by nutriosomes thanks to the association of the prebiotic dextrin and the antioxidant curcumin.

Overall results suggest that curcumin nutriosomes represent a promising tool for the intestinal treatment of oxidative stress injuries, and they can be proposed for the development of functional

foods, dietary supplements, and pharmaceutical preparations thanks to their easy preparation method, biocompatibility and promising performances *in vivo*.

ACKNOWLEDGMENTS

SAXS experiments were performed at the BL11-NCD beamline of the ALBA Synchrotron facility with the collaboration of ALBA staff. The beam-time at ALBA was kindly provided within the approved proposal n. 2013110789. The research leading to these results has received funding from the European Community's Seventh Framework Program (FP7/2007-2013) under the grant agreement n. 312284.

References

1. G.R.Gibson, J Clin Gastroenterol. 2008 Jul;42 Suppl 2:S75-9.
2. G.H. Norman, Annu Rev Nutr. 2008;28:215-31.
3. Z. Huyut, Ş. Beydemir, İ, Gülçin. Biochem Res Int. 2017;2017:7616791.
4. S.j.Hewlings, D.S. Kalman, Foods. 2017 Oct 22;6(10). pii: E92.
5. R.F. Tayyem, D.D. Heath, W.K. Al-Delaimy. C.L. Nutr. Cancer. 55 (2006) 126–31.
6. H. Hatcher, R. Planalp, J. Cho, F.M. Torti, S. V Torti. Cell. Mol. Life Sci. 65 (2008) 1631–52.
7. W. Wongcharoen, A. Phrommintikul, Int. J. Cardiol. 133 (2009) 145–51.
8. R.K. Maheshwari, A.K. Singh, J. Gaddipati, R.C. Srimal, Life Sci. 78 (2006) 2081–2087.
9. B.B. Aggarwal, K.B. Harikumar, Int. J. Biochem. Cell Biol. 41 (2009) 40–59.
10. H. Hanai, T. Iida, K. Takeuchi, F. Watanabe, Y. Maruyama, A. Andoh, T. Tsujikawa, Y. Fujiyama, K. Mitsuyama, M. Sata, M. Yamada, Y. Iw aoka, K. Kanke, H. Hiraishi, K. Hirayama, H. Arai, S. Yoshii, M. Uchijima, T. Nagata, Y. Koide, Clin. Gastroenterol. Hepatol. 4 (2006) 1502–6.
11. D. Patra, D. Ahmadieh, R. Aridi, Colloids Surf. B. Biointerfaces. 110 (2013) 296–304.
12. M. Mehanny, R.M. Hathout, A.S. Geneidi, S. Mansour, J. Control. Release. 225 (2016) 1–30.
13. P. Ramalingam, S.W. Yu, Y.T. Ko, Food Res. Int. 84 (2016) 113–119.
14. M.L. Manca, J.E. Peris, V. Melis, D. Valenti, M.C. Cardia, D. Lattuada, E. Escribano-Ferrer, A.M. Fadda, M. Manconi, RSC Adv. 5 (2015) 105149–105159.
15. J. Li, I.W. Lee, G.H. Shin, X. Chen, H.J. Park, Eur. J. Pharm. Biopharm. 94 (2015) 322–32.
16. S. Kim, R. Diab, O. Joubert, N. Canilho, A. Pasc, Colloids Surf. B. Biointerfaces. 140 (2016) 161–8..
17. A. Patel, Y. Hu, J.K. Tiwari, K.P. Velikov, Soft Matter. 6 (2010) 6192. doi:10.1039/c0sm00800a.
18. C. Caddeo, O. Díez-Sales, R. Pons, C. Carbone, G. Ennas, G. Puglisi, A.M. Fadda, M. Manconi, J. Colloid Interface Sci. 461 (2016) 69–78. doi:10.1016/j.jcis.2015.09.013.
19. M.A. Akl, A. Kartal-Hodzic, T. Oksanen, H.R. Ismael, M.M. Afouna, M. Yliperttula, A.M. Samy, T. Viitala, J. Drug Deliv. Sci. Technol. 32 (2016) 10–20. doi:10.1016/j.jddst.2016.01.007.
20. R.N. Rowland, J.F. Woodley, Biochim. Biophys. Acta. 620 (1980) 400–9.
21. W. Liu, A. Ye, W. Liu, C. Liu, J. Han, H. Singh, Food Chem. 175 (2015) 16–24. doi:10.1016/j.foodchem.2014.11.108.
22. C. Li, Y. Zhang, Su, Feng, Long, Z. Chen, Int. J. Nanomedicine. Volume 7 (2012) 5995. doi:10.2147/IJN.S38043.
23. G. Chen-yu, Y. Chun-fen, L. Qi-lu, T. Qi, X. Yan-wei, L. Wei-na, Z. Guang-xi, Int. J. Pharm. 430 (2012) 292–298. doi:http://dx.doi.org/10.1016/j.ijpharm.2012.03.042.
24. M.L. Manca, I. Castangia, M. Zaru, A. Nácher, D. Valenti, X. Fernàndez-Busquets, A.M. Fadda, M. Manconi, Biomaterials. 71 (2015) 100–9. doi:10.1016/j.biomaterials.2015.08.034.
25. M. Manconi, J. Aparicio, A.O. Vila, J. Pendàs, J. Figueruelo, F. Molina, Colloids Surfaces A Physicochem. Eng. Asp. 222 (2003) 141–145.
26. C. Mura, A. NÃ¡cher, V. Merino, M. Merino-Sanjuan, C. Carda, A. Ruiz, M. Manconi, G. Loy, A.M. Fadda, O. Diez-Sales, Int. J. Pharm. 416 (2011) 145–154.
27. D.G. Fatouros, S.G. Antimisiaris, J. Colloid Interface Sci. 251 (2002) 271–7. doi:10.1006/jcis.2002.8432.
28. W. Liu, W. Liu, A. Ye, S. Peng, F. Wei, C. Liu, J. Han, Food Chem. 196 (2016) 396–404. doi:10.1016/j.foodchem.2015.09.050.
29. M. Manconi, J. Aparicio, D. Seyler, A.O. Vila, J. Figueruelo, F. Molina, Colloids Surfaces

A Physicochem. Eng. Asp. 270-271 (2005) 102–106.
30. S. Rao, C.A. Prestidge, Expert Opin. Drug Deliv. (2016) 1–17. doi:10.1517/17425247.2016.1151872.
31. M. Manconi, S. Mura, M.L. Manca, A.M. Fadda, M. Dolz, M.J. Hernandez, A. Casanovas, O. Díez-Sales, Int. J. Pharm. 392 (2010) 92–100.
32. M.J. Barea, M.J. Jenkins, M.H. Gaber, R.H., Int. J. Pharm. 402 (2010) 89–94. doi:10.1016/j.ijpharm.2010.09.028.
33. M. Tanaka, A. Hosotani, Y. Tachibana, M. Nakano, K. Iwasaki, T. Kawakami, T. Mukai, Langmuir. 31 (2015) 12719–26. doi:10.1021/acs.langmuir.5b03438.
34. D. Grizard and C. Barthomeuf, Reprod. Nutr. Dev., 1999, 39, 563–588.
35. J. W. Anderson, B. M. Smith and N. J. Gustafson, Am. J. Clin. Nutr., 1994, 59, 1242S–1247S.
36. I. I. Ivanov and K. Honda, Cell Host Microbe, 2012, 12, 496–508.
37. L. Guerin-Deremaux, F. Ringard, F. Desailly, D. Wils, W. Timm, Y. Açil, C. Glüer, J. Schrezenmeir, C. Bouteloup-Demange and Y. Rayssiguier, Nutr. Res. Pract., 2010, 4, 470.
38. W. Pasman, D. Wils, M.-H. Saniez and A. Kardinaal, Eur. J. Clin. Nutr., 2006, 60, 1024–1034.
39. I. Castangia, A. Nácher, C. Caddeo, V. Merino, O. Díez-Sales, A. Catalán-Latorre, X. Fernàndez-Busquets, A. M. Fadda and M. Manconi, Acta Biomater., 2015, 13, 216–27.
40. A. R. Martín, I. Villegas, C. La Casa and C. Alarcón De La Lastra, Biochem. Pharmacol., 2004, 67, 1399–1410.
41. E. O. Farombi, I. A. Adedara, B. O. Ajayi, O. R. Ayepola and E. E. Egbeme, Basic Clin. Pharmacol. Toxicol., 2013, 113, 49–55.
42. G. Serreli, A. Incani, A. Atzeri, A. Angioni, M. Campus, E. Cauli, R. Zurru and M. Deiana, J. Food Sci., 2017, 82, 380–385.
43. E. Blanco-García, F. J. Otero-Espinar, J. Blanco-Méndez, J. M. Leiro-Vidal and A. Luzardo-Álvarez, Int. J. Pharm., 2017, 518, 86–104.
44. J. S. Lee, H. W. Kim, D. Chung and H. G. Lee, Food Hydrocoll., 2009, 23, 2226–2233.
45. C. Caddeo, R. Pons, C. Carbone, X. Fernàndez-Busquets, M. C. Cardia, A. M. Maccioni, A. M. Fadda and M. Manconi, Carbohydr. Polym., 2017, 157, 1853–1861.
46. C. Mura, A. Nacher, V. Merino, M. Merino-Sanjuan, C. Carda, A. Ruiz, M. Manconi, G. Loy, A. M. Fadda and O. Diez-Sales, Int. J. Pharm., 2011, 416, 145–154.
47. Manconi, M., Isola, R., Falchi, A.M., Sinico, C., Fadda, A.M., 2007. Intracellular distribution of fluorescent probes delivered by vesicles of different lipidic composition. Colloids and Surfaces B: Biointerfaces 57, 143-151.
48. I. Castangia, A. Nácher, C. Caddeo, D. Valenti, A. M. Fadda, O. Díez-Sales, A. Ruiz-Saurí and M. Manconi, Acta Biomater., 2014, 10, 1292–1300.
49. M. Manconi, M. L. Manca, D. Valenti, E. Escribano, H. Hillaireau, A. M. Fadda and E. Fattal, Int. J. Pharm., 2017, 525, 203–210.
50. W.-C. Hung, F.-Y. Chen, C.-C. Lee, Y. Sun, M.-T. Lee and H. W. Huang, Biophys. J., 2008, 94, 4331–4338.
51. I. Castangia, M. L. Manca, P. Matricardi, C. Sinico, S. Lampis, X. Fernàndez-Busquets, A. M. Fadda and M. Manconi, Int. J. Pharm., 2013, 456, 1–9.
52. M. L. Manca, I. Castangia, P. Matricardi, S. Lampis, X. Fernàndez-Busquets, A. M. Fadda and M. Manconi, Colloids Surf. B. Biointerfaces, 2014, 117, 360–367.
53. H. K. Syed, K. Bin Liew, G. O. K. Loh and K. K. Peh, Food Chem., 2015, 170, 321–326.
54. M. Manconi, J. Pendas, Ledon, N, T. Moreira, C. Sinico, L. Saso and A. M. Fadda, J. Pharm. Pharmacol., 2009, 61, 423–430.
55. S. Sen and R. Chakraborty, 2011, pp. 1–37.
56. H. H. . Cohly, A. Taylor, M. F. Angel and A. K. Salahudeen, Free Radic. Biol. Med., 1998, 24, 49–54.

57. X.-C. Zhao, L. Zhang, H.-X. Yu, Z. Sun, X.-F. Lin, C. Tan and R.-R. Lu, Food Chem., 2011, 129, 387–394.
58. R. K. Maheshwari, A. K. Singh, J. Gaddipati and R. C. Srimal, Life Sci., 2006, 78, 2081–2087.
59. Y. Sambuy, I. De Angelis, G. Ranaldi, M. L. Scarino, A. Stammati and F. Zucco, Cell Biol. Toxicol., 2005, 21, 1–26.
60. P. Anand, A. B. . Kunnumakkara, R. A. . Newman and B. B. . Aggarwal, Bioavailability of Curcumin: Problems and Promises, http://pubs.acs.org/doi/pdf/10.1021/mp700113r, (accessed 9 March 2015).
61. M.-H. Pan, T.-M. Huang and J.-K. Lin, Drug Metab. Dispos.
62. V. Ravindranath and N. Chandrasekhara, Toxicology, 1980, 16, 259–265.
63. R. A. Sharma, C. R. Ireson, R. D. Verschoyle, K. A. Hill, M. L. Williams, C. Leuratti, M. M. Manson, L. J. Marnett, W. P. Steward and A. Gescher, Clin. Cancer Res., 2001, 7, 1452–8.
64. J. Shaikh, D. D. Ankola, V. Beniwal, D. Singh and M. N. V. R. Kumar, Eur. J. Pharm. Sci., 2009, 37, 223–230.
65. F. Akhtar, M. M. A. Rizvi and S. K. Kar, Biotechnol. Adv., 2012, 30, 310–320.
66. K. Maiti, K. Mukherjee, A. Gantait, B. P. Saha and P. K. Mukherjee, Int. J. Pharm., 2007, 330, 155–163.
67. M. Takahashi, S. Uechi, K. Takara, Y. Asikin and K. Wada, J. Agric. Food Chem, 2009, 57, 9141–9146.
68. N. Hussain, Adv. Drug Deliv. Rev., 2001, 50, 107–142.